1-1-1977

A mathematical model for the evolution of fluoride-containing fumes from the aluminum reduction cell.

Jonathan P. Dandridge

A MATHEMATICAL MODEL FOR THE EVOLUTION OF FLUORIDE-CONTAINING FUMES FROM THE ALUMINUM REDUCTION CELL

by

Jonathan P. Dandridge

A Thesis

Presented to the Graduate Committee

of Lehigh University

in Candidacy for the Degree of

Master of Science

in

Metallurgy and Materials Science

Lehigh University

1977

Certificate of Approval

This thesis is accepted and approved in partial fulfillment of the requirements for the degree of Master of Science.

6 September 1977
(date)

Professor in Charge

Chairman of Department

Acknowledgements

I would like to thank all those who assisted in the preparation of this thesis. I am especially grateful to Dr. Walter C. Hahn, my thesis advisor, for his guidance in the preparation of the model and writing of the thesis, and his encouragement at difficult points in the project. I am also indebted to Dr. Stephen K. Tarby and the Chemical Metallurgy Program for support of my research and graduate studies.

Thanks are also due to Mr. W. E. Haupin, Mr. C. M. Marstiller, and Dr. W. Wahnsiedler of Alcoa Research Laboratories for their assistance in technical matters, location of reference material, and provision of experimental correlations for the thesis.

I am also grateful to members of the Lehigh University Department of Metallurgy and Materials Science especially my colleagues and especially Alton D. Romig, Jr., Chester J. Van Tyne, and Philip C. Wingert for their help and moral support during this project, and Louise Valkenburg for preparing the final copy of the thesis.

TABLE OF CONTENTS

List of Tables

List of Figures

Abstract

A mathematical model was developed that calculates fluoride evolution from aluminum reduction cells as a function of bath temperature, bath composition, water content of alumina, and anode hydrogen content. This model uses both theoretical concepts and the results of measurements on experimental cells as a basis for the model equations. Different hypotheses for fluoride evolution mechanisms were investigated and alternative ways to express these mechanisms developed. These include: use of vapor pressure data of either Kuxmann and Tillessen or Vajna and Bacchiega to model vaporization of bath, using percent of entrainment value of Haupin or Less and Waddington, assumption of HF generation by atmospheric moisture entering the cell, use of kinetic factor for HF generation by anode hydrogen, and determination of whether water contained in feed alumina reacts to form HF to the extent of a constant value of 0.1 weight percent water or 5 percent of water content upon entering the bath.

The model was tested by comparing the results to values calculated from regression equations derived from 3 sets of experimental measurements. These results show that the optimum correlations exist when the vapor pressure data of Kuxmann and Tillessen, the use of a kinetic factor for anode hydrogen, and assumption of alumina water reacting to the extent of 5 percent are used in the

model. No conclusion could be drawn as to the optimum entrainment figure. The results also indicate that the optimum correlation resulted from not using the atmospheric moisture mechanism for HF evolution, but that this mechanism appears to be a significant mechanism for HF evolution.

Introduction

The Operation of the Aluminum Reduction Cell

Virtually all of the aluminum metal commercially produced today is made by electrolytic reduction of alumina with the Hall-Heroult cell. Essentially the process can be described as the reduction of aluminum oxide in solution by carbon, the driving force for the reaction being provided by the cell potential. The electrolyte used is cryolite (Na_3AlF_6) which has the unique property of being able to dissolve up to about 11.5 weight percent alumina, and thus makes the process feasible.

The reduction cell is constructed of an insulated steel box lined with carbon, providing a container for the highly reactive cryolite and acting as the cathode for the cell. Carbon anodes are suspended above the cell on steel bus bars. The carbon anodes are normally consumed at a rate of about 2.5 cm. per day[1] and therefore a mechanism must exist for their replenishment. One method is to use replaceable carbon blocks, formed and prebaked in a furnace, which are renewed as needed. Normally about 24 to 26 of these anodes per cell are used. An alternative method, more popular in Europe, is the Söderberg electrode, which consists of a container open at top and bottom, into which carbon paste is fed continuously. The paste is baked by the heat of the cell and thus the anode feeds continuously.

The cell normally operates at a temperature of about 1230K. During normal operation the bath material on the top of the cell

solidifies and forms a crust over the cell. The alumina feed to the cell is charged on top of the crust. In order to keep the cell alumina concentration at the normal value of 4 to 5 weight percent, the crust is broken periodically and the alumina stirred into the bath. If the alumina concentration is allowed to get too low (below about 2 percent) the so-called "anode effect" occurs. At this concentration a film of fluorine gas forms around the anode which increases the cell resistance and causes a dramatic increase in cell voltage. The anode effect is extinguished by breaking the crust and stirring in alumina.

The bath used in the cell is generally not pure cryolite but usually contains excess aluminum fluoride and other additions including calcium fluoride, magnesium fluoride, and other halide salts which are added principally to lower the bath melting temperature and adjust cell conductivity. The amount of aluminum fluoride present is usually expressed as "cryolite ratio" defined as the ratio of mole fraction sodium fluoride to mole fraction aluminum fluoride, cryolite being treated as though it were dissociated completely. Thus pure cryolite has a cryolite ratio of 3.0.

The aluminum metal produced is heavier than cryolite and collects at the bottom of the cell. It is siphoned from the cell at periodic intervals.

From the reduction of alumina by the anode carbon, carbon dioxide gas is produced which bubbles up to the cell surface and escapes through holes in the crust. Some carbon monoxide is usually

produced by secondary reactions that reduce some of the carbon dioxide. For a normal cell efficiency of 85 percent (85 percent of the theoretical aluminum production predicted by Faraday's law) approximately 0.4 kg of anode carbon is consumed and 732 liters of CO_2 and CO gas produced for each kilogram aluminum produced.

Fluoride Evolution Mechanisms

During electrolysis, in addition to the CO and CO_2 gas given off, fluoride-containing fumes are evolved. This evolution of fumes has been a concern of aluminum producers due to employee health hazards, environmental standards, and resulting operating problems.

Several studies have been made of the nature of the fluoride fume.[2,3] It has been found to consist of a gaseous component, mostly HF with some CF_4 and other fluorides, and a particulate component made up of several solid fluoride species, mostly $NaAlF_4$ and cryolite. This describes the fluoride fume at the point of leaving the cell. The types of fumes and their proportions may be altered by secondary reactions once the fumes leave the cell. These secondary reactions, however, do not alter the overall fluoride balance and therefore will not be considered in this report except as they affect interpretations of measurements made of fluoride evolution in operating cells.

Three principal mechanisms for fluoride evolution have been proposed by investigators to account for these various types of fumes:

1. Vaporization of the fluoride containing electrolyte components and subsequent entrainment of the vapor in

the anode gas.

2. Entrainment of particles of the electrolyte in the anode gas.
3. Formation of fluoride gases (primarily HF) by reactions within the cell.

Each of these mechanisms will be discussed individually in the succeeding sections.

Vaporization Mechanism

The vaporization mechanism has been extensively investigated and is thought to be well understood. In melts of NaF-$Al F_3$ mixtures, the vapor species have been found[4] to consist of sodium tetrafluoroaluminate ($NaAlF_4$) with smaller amounts of another component with a heavier molecular weight. Many researchers[2,5] have concluded this component is the dimer $Na_2Al_2F_8$ although this has been disputed[6] due to possible discrepancies in the dimerization assumption. However, the discrepancies could be due to experimental error and the calculations of fluoride content of the vapor could be affected little by a variation in the assumption of a different type of heavier molecule (for example, $NaAl_2F_7$ has been suggested[6]) since the dimer component is relatively small to begin with. Therefore for this model the volatile components were assumed to be $NaAlF_4$ and $Na_2Al_2F_8$. The concentration of these components in the anode gas can then be determined from the calculated equilibrium vapor pressures.

Entrainment Mechanism

The mechanism of entrainment of bath particles is the

least understood of the mechanisms. Less and Waddington,[7] upon investigating the composition of dust contained in unburned cell fumes, found that the dust was composed of a fine and a coarse fraction. Unburned refers to the fact that the fumes were collected directly from cell openings with little opportunity for reaction with air or atmospheric moisture to occur. The fine fraction is composed of chiolite ($Na_5Al_3F_{14}$) which is the condensed form of the vapor above molten cryolite, $NaAlF_4$ being unstable below about 973 K. The coarse fraction is principally composed of cryolite, alumina, and carbon particles. Since a vapor of the composition Na_3AlF_6 has not been observed ($NaAlF_4$ being the observed vapor phase as previously noted) it appears that these components must originate directly from the cell. It is theorized that cell gases formed at the anodes bubble through the bath and droplets are formed as the bubbles break the surface. These droplets are then carried upwards in the air stream from the cell. This would account for the particles observed. The only other likely source for cryolite would be the hydrolysis of $NaAlF_4$ vapor as in the reaction: $NaAlF_4(g) + H_2O(g) = \frac{1}{3} Na_3AlF_6\ (s) + \frac{1}{3} Al_2O_3\ (s) + 2\ HF(g)$ but since the measurements of Less and Waddington were made on unburned fumes with little opportunity for contact with air and subsequent reaction, it seems to be a reasonable assumption that the relative proportions of fluorides in fine and coarse dust represent fume evolution from bath vaporization and bath entrainment respectively.

In addition to Less and Waddington, other workers have made estimates of fluoride evolution due to entrainment by measuring

the components given off. A different technique which may hold promise for future more accurate measurements of entrainment involves analysis of calcium content of the particulate fume.[8] These various estimates of entrainment are summarized in Table 1:

TABLE 1

Fluoride Evolution Attributable to Entrainment

Investigator	Ref.	Percent of evolution due to entrainment	Basis of analysis
Less and Waddington	7	17 - 23%	cryolite content
Miller	9	10 - 20%	cryolite content
Haupin	8	6 - 7%	calcium content
Andes, Bjorke, and Farrier	10	29%	cryolite content

From what is already known of the entrainment mechanism, a variation of entrainment with cell parameters such as temperature and composition might be expected. Workers at Alcoa[11] have qualitatively observed increasing entrainment with increasing alumina concentration. Studies of entrainment in chemical engineering processes[12] show that entrainment varies approximately as the cube of gas velocity for entrainment ratios (kg. liquid entrained/kg. vapor) at the level found in aluminum cells. The same work also notes that entrainment varies with the surface tension of the liquid. Extensive data for the surface tension of cryolite baths and their variation with cell parameters are available[13] from which can be predicted qualitatively a variation of entrainment with cryolite ratio,

temperature, and bath additions. However, at the present time no quantitative data exists that shows the variation of fluoride fume entrained with variations in cell parameters. This matter will be dealt with further upon development of and discussion of the fluoride evolution model.

HF Evolution Mechanisms

During normal cell operation (outside of "anode effects") roughly one-third of the fluoride evolution is accounted for by hydrogen fluoride generation within the cell. This generation appears to be due to reactions between hydrogen and the fluoride constituents of the bath, such as cryolite and aluminum fluoride. Several sources have been proposed for the hydrogen that takes part in these reactions. Water vapor from the potroom atmosphere, water contained in the alumina feed to the cell, and hydrogen contained in the anodes are three that are considered the principal sources.

HF evolution due to potroom moisture is the first mechanism to be considered. This moisture presumably is carried into the cell by air being drawn under the crust. At first it might seem doubtful that air would be present in much quantity underneath the cell crust. However, measurements by Henry[14] indicate that nitrogen and argon are present in the anode gas in proportion to their concentration in the atmosphere which suggests some air does enter the cell and therefore there is an opportunity for atmospheric moisture to react.

So far experiments to investigate this hypothesis have been inconclusive. Henry[14] conducted measurements of HF evolution from experimental cells over the course of several weeks. His data

taken over a range of humidity values showed no significant correlation between humidity and HF evolution. However, before rejecting this mechanism, it should be noted that the range of humidity values was small and if fluoride evolution by this mechanism was significant but small, a correlation could easily be masked by variations in other cell variables or experimental error. Henry demonstrated that the latter could be 10 percent by making two separate sets of readings on cells running under similar conditions. Therefore this mechanism should still be considered significant until further experimental work demonstrates otherwise.

The alumina feed is another possible source of water. Alumina is charged to the surface of the cell where it remains on the crust until the crust is broken and the alumina stirred into the bath. According to Henry's data[14] for moisture loss of alumina, the water content should be at 0.2 to 0.5 weight percent before break-in. However, if all of this water were to react, the HF evolution would be far in excess of that measured.

Some experiments by Henry[14] provide some theories to account for this fact. When samples of alumina of varying water content were fed directly into the bath, about 5 percent of the water reacted to form hydrogen fluoride. However, when samples of alumina of varying water content were fed onto the crust in the usual way, the evolution remained essentially constant at a value that would be the equivalent of 0.1 weight percent water in the alumina completely reacting. Henry warns that these data are only accurate within 10 percent, an accuracy that could mask differences

in evolution due to water content if only 5 percent of the water reacts. For example, a water content of 0.1 weight percent would then contribute 0.2 g. HF/kg Aℓ while alumina of 2.0 weight percent would contribute 4 g. HF/kg Aℓ. An error of 10 percent would represent 2 g/kg, a large enough error to mask this contribution. Therefore, it is possible that a variation of fluoride emission with varying water content of alumina feed does exist.

The last source of hydrogen to be considered is adsorbed hydrogen or hydrocarbons within the carbon anodes. A direct reaction of this hydrogen with the melt to produce HF is not thermodynamically feasible. However, the hydrogen could be oxidized to water, which would then react as previously discussed. Two water formation reactions have been proposed. Kostyukov[15] proposed the reaction

$$H_2(g) + CO_2(g) = H_2O(g) + CO(g) \quad \Delta G^{o}_{1300^{o}K} = -6028 \text{ j/mole}$$

However, Grjotheim[2] argues that this reaction may not occur due to electrostatic repulsion between CO_2 gas bubbles and the anode surface, where this reaction would be likely to take place. He proposes as an alternative that hydrogen is electrochemically oxidized to water, the cell potential of a typical pot cell being sufficient to drive this reaction. Since this reaction would involve an oxide ion such as an ion of alumina or one of its complexes, the kinetic barrier proposed by Grjotheim for Kostyukov's reaction would not exist here. At present there is insufficient evidence to support any particular mechanism for the oxidation of hydrogen. However, data from Henry[14] indicates that kinetics have to be considered

since his experiments appear to show that about one-half of the available hydrogen reacts to form hydrogen fluoride. This factor will be discussed in more detail when the development of the fluoride model is dealt with.

Work Done to Date on Fluoride Evolution

Until now, previous attempts to model fluoride evolution have been primarily empirical correlations of fluoride evolution data as a function of cell parameters. The lack of attempts to model evolution on a theoretical basis is undoubtedly a result of the complexity of the process and the difficulty of procuring reliable data due to the complexity of the cryolite-alumina system and the proprietary nature of many industrial operations.

The first comprehensive attempt to study fluoride evolution was by Henry[14] who published a study in 1963 conducted using 10,000 ampere experimental cells. One result of his work was a correlation of fluoride evolution as a function of temperature, cryolite ratio, and alumina concentration.

The first generally available correlation of fluoride evolution in industrial cells was that of Solntsev[3] published in 1967 which gives evolution measured in Russian industrial cells as a function of temperature and cryolite ratio. The equation developed from his data is:

$$WFSOL = \frac{279}{(CRATIO)^2} + 0.047\ (T - 273) - 61$$

The symbols used here and throughout this report are identical to those used as FORTRAN variable names in the model. A table of these

symbols is reproduced in Appendix 1.

An attempt to look at the mechanisms causing fluoride evolution was made by Grjotheim, Kvande, Motzfeldt, and Welch.[2] Their survey paper includes a modelling of the evolution of fluoride due to vaporization of the bath and a discussion of other mechanisms.

It would then appear that a next step in the study of fluoride evolution would be to try to use known theoretical concepts along with experimental measurements to create a more comprehensive model that would go beyond the empirical correlations. This leads to the purpose of this work which, it is hoped, will make a modest start toward this next step in fluoride evolution studies.

Objective

The objective of this project is to develop a mathematical process model that will express fluoride evolution as a function of several important cell parameters. These parameters include

- bath temperature
- bath composition - includes:
  - cryolite ratio (moles NaF/moles AlF_3)
  - alumina content
  - CaF_2 content
- water content of alumina
- anode hydrogen content

The theoretical considerations discussed in the introduction together with available experimental measurements are used to develop the mathematical relations used. This process model, referred to in

this work as FLORIDE, is written in FORTRAN IV and is designed to be compatible with available cell models. A source listing for this model is included in Appendix 2.

In addition to the development of the model itself, the objectives include:

1. Investigating different proposed theories for the fluoride evolution mechanisms and alternative ways to express the mechanisms to determine the optimum algorithms for the model.
2. Investigating the state of the art in modelling fluoride evolution and suggesting areas for further investigation that would allow a more accurate and comprehensive model to be constructed.

Source of Experimental Data

At the present time, few comprehensive measurements of fluoride evolution as a function of cell parameters exist in the literature. However, at least 3 mathematical correlations do exist that can be used as a basis of comparison, keeping in mind that use of these equations involves a loss in accuracy over actual experimental data points. The first is Solntsev's correlation[3] previously cited. It is limited due to the fact that it only includes temperature and cryolite ratio as variables. A more comprehensive correlation is that by Haupin[8] of Alcoa which includes temperature, cryolite ratio, percent water in alumina, anode hydrogen content, atmospheric humidity, and bath alumina content. Although Haupin's correlation includes all of the variables

(except calcium fluoride content) that are included in the model, it is limited by being only a linear regression with a multiple correlation coefficient r^2 of 0.58 (corrected for 11 degrees of freedom). This value of correlation coefficient indicates a fair amount of scatter in the data, which is to be expected since these measurements were made on industrial cells in normal operation, far removed from the ideal laboratory situation. This must be taken into account when using this equation as a basis for comparison. The same paper by Haupin also includes a correlation of Henry's data[14] which gives fluoride evolution as a function of temperature, cryolite ratio, alumina concentration, and water content of alumina. It should be noted that the data for this correlation were taken on an experimental laboratory cell and although this may have resulted in more accurate measurements than are possible in measurements on industrial cells (such as the measurements by Solntsev and Haupin), the correlation may not be totally representative of behavior to be expected in industrial practice, since other factors such as size, magnetic effects, current, etc. may affect the outcome. Therefore all of the above correlations have their drawbacks and it is hoped that in future actual "hard data" will be available to give a better comparison for future modelling efforts.

Procedure

It is evident from the previous discussion that fluoride evolution is dependent upon several cell parameters including bath composition and temperature. These in turn normally vary during the cell operation due to the reactions within the cell to produce aluminum metal and byproducts, periodic additions of alumina and other bath materials, and variations brought about by changes in operating conditions, such as the anode effect. Therefore, an ideal way to provide realistic inputs to FLORIDE would be to use a dynamic model of the aluminum cell to generate values for the bath temperature, composition, and other parameters. Unfortunately, at this time, no generally available dynamic cell model exists that could be used for this project. However, FLORIDE is written so that if such a model became available, it would be a simple matter to link the fluoride model to it.

Since such a model is not available at the present time, it was decided to use a simpler static model of the cell in which temperature and composition remain constant over time. This model would calculate the parameters of anode gas evolution rate and anode consumption, which are inputs to FLORIDE.

Static models available include a model developed by Revere Copper and Brass,[16] and a more theoretical model developed by Morris.[17] The former was chosen for this project because it is the most complete and is available in the literature in the detail necessary to be put on the computer with a minimum amount of work.

The equations given by Richard for bath conductivity and heat

losses were used to calculate the total heat loss from the bath. Current efficiency was then calculated using an iterative technique that used heat loss, reaction voltage, cell voltage, and bath conductivity. Most of these equations were from Richard's work, except that a formula from Berge, Grjotheim, Krohn, Neumann, and Tørklep[18] was used to calculate an initial guess for current efficiency. Moles of anode gas and anode consumption were calculated using the equations:

$$Al_2O_3 + \frac{3}{2} C = 2\ Al + \frac{3}{2} CO_2$$

$$3(1 - CE)CO_2 + 2(1 - CE)Al = (1 - CE)Al_2O_3 + 3(1 - CE)CO$$

to derive the following relations:

NANGAS = 27.7984/CE

ACONS = 0.333887/CE

This then provides the fluoride model, subroutine FLORIDE, all of the cell variables that are needed to calculate fluoride evolution. Temperature and bath composition are also passed from the cell model. Although in this particular cell model they are fixed for a given run, this would allow them to be varied if a dynamic cell model were substituted without requiring a change of subroutine FLORIDE.

Development of the Fluoride Evolution Model

FLORIDE is a subprogram that generates a value for cell fluoride evolution (in grams fluorine per kilogram aluminum produced) using equations based upon the mechanisms discussed in the introduction. These mechanisms are divided into 3 types--bath vaporization, bath entrainment, and HF generation mechanisms--and are discussed separately in the following section.

Vaporization

The modelling of fluoride evolution due to vaporization of bath is straightforward. Each mole of gas evolved from the cell is assumed to contain an amount of fluoride vapor equivalent to its equilibrium partial pressure. This is reasonable since the gas is bubbled through the electrolyte and under a crust of frozen electrolyte thus allowing ample opportunity for saturation. The moles of gas evolved per kilogram aluminum produced is obtained from the cell model. The equilibrium partial pressure of vapor above the melt must then be calculated.

As previously mentioned, the vapor species above molten NaF-AlF_3 mixtures is believed to be predominantly $NaAlF_4$ with smaller amounts of $Na_2Al_2F_8$ dimer. Kuxmann and Tillessen[19] made measurements of vapor pressure above NaF-AlF_3 mixtures of varying composition. These data are among the more recent and appear to agree well with measurements made by others.[20,21,22] Their data were fitted to curves of the form:

$$\log_{10} P = - A/T + B$$

The coefficients A and B are given for several compositions of the mixture. These data are reproduced in Table 2.

TABLE 2[19]

Vapor Pressure above NaF-AlF_3 Mixtures (in Pascals)

$\log_{10}P = 133.322\ (-A/T + B)$

Concentration Weight Percent NaF	AlF_3	Cryolite Ratio Moles NaF/Moles AlF_3	Constants A	B	Temp. Range Kelvin
40	60	3.00	10399	8.695	1281 - 1473
42	58	2.76	10107	8.569	1281 - 1473
50	50	2.00	9491	8.478	1218 - 1473
60	40	1.34	8842	8.304	995 - 1473
66.7	33.3	1.00	8568	8.247	1152 - 1473
70	30	0.86	8239	8.175	1290 - 1473

In order to transform this table to a form more suited to the model, the values for A and B were fitted to a least squares line,[23] as a function of cryolite ratio, with the following results:

$$A = 950.86\ (CRATIO) + 7537.4,\ r^2 = .9929$$

$$B = 0.21974\ (CRATIO) + 8.0099,\ r^2 = .9774$$

This then gives an expression for vapor pressure as a function of temperature and composition of the mixture in terms of cryolite ratio (moles NaF/moles AlF_3). What remains is to convert from concentration of fluoride vapor to grams of fluorine per kilogram of aluminum produced. This requires knowledge of the composition of the vapor. Using the assumption of a vapor primarily composed of $NaAlF_4$ with smaller amounts of $Na_2Al_2F_8$ dimer, the atoms of fluorine per mole fluoride vapor would be 4(1 + FDIMER) where FDIMER is the atomic fraction of the dimer. The equilibrium constant for the monomer-dimer reaction:

$$2\ NaAlF_4 = Na_2Al_2F_8$$

has been expressed by the following relation:

$$\log_{10}(KVAPR) = 9300/T - 5.9$$

if FDIMER = p_d/PVAPR and KVAPR = $p_d/(PVAPR-p_d)^2$ where p_d is the partial pressure of dimer, then

$$KVAPR = \frac{(PVAPR)(FDIMER)}{[PVAPR-(PVAPR)(FDIMER)]^2}$$

Solving for FDIMER yields:

$$FDIMER = \frac{2(KVAPR)(PVAPR) + 1 - \sqrt{4(KVAPR)(PVAPR) + 1}}{2(KVAPR)(PVAPR)}$$

The fluoride evolution due to bath vaporization is then given by:

$$WFVAPR = (FVP)(PVAPR)(NANGAS)(1 + FDIMER)(75.99)$$

FVP is a factor for vapor pressure to allow for the fact that alumina and calcium fluoride are present in the bath thus lowering the vapor pressure. From Henry's data[14] on bath volatility this is calculated to be 0.6 for a typical operating condition of 4% alumina and 8% calcium fluoride. The first 3 terms in the equation give the moles of $NaAlF_4$ per kilogram aluminum produced. This is multiplied by 4 (gm-atoms fluorine per mole $NaAlF_4$) times the fraction of dimer times 18.998 (grams fluorine per gram atom). The use of the factor 0.6 to account for alumina and calcium fluoride content is obviously an approximation and has the disadvantage of not allowing the effect of varying these quantities on fluoride evolution to be investigated.

While the measurements of Kuxmann and Tillesen are thorough, including a range of temperatures and cryolite ratios, they do not include measurements made at varying concentrations of alumina and

calcium fluoride. Vapor pressure data are available from Vajna and Bacchiega[24] which include these variations. However their data are not as comprehensive and unfortunately the two sets of data do not completely agree, preventing them from being combined into one correlation. Therefore a separate correlation of Vajna and Bacchiega's measurements was derived using a multiple linear regression technique. Log vapor pressure was regressed against inverse temperature, the other terms being linear. This was found to improve the correlation. The resultant expression is:

$$\log_{10}P = (10.168\text{-}11105.8(\frac{1}{T}) - 0.03438\ \text{NAL203} - 0.03302\ \text{NCAF2}$$

$$-0.37494\ \text{CRATIO}) \quad (r^2 = .9575)$$

This equation was then incorporated as an option in the model to investigate the effects of varying alumina and calcium fluoride concentration on fluoride evolution.

Entrainment

The second mechanism of fluoride evolution, the entrainment of particles of the bath, is more difficult to handle. As discussed in the introduction, estimates of bath entrainment vary from 7 to 20 percent of total fluoride evolution depending upon the method of measurement used. Variations of entrainment with cell parameters can can be inferred from the variations in bath surface tension and gas evolution rate. However, since correlations between these factors and entrainment are not known and the application of a theoretical model would be complex and hazardous at best, the best approach at present is to estimate the fluoride evolution due to entrainment

for typical cell operation, and use this value in the model as a constant. Less and Waddington's[7] estimates, which appear to be the most reliable, show 19 percent of the emission attributable to entrainment during normal cell operation. A figure for total fluoride evolution for typical cell conditions (cryolite ratio 2.4 - 3.0, temperature 1244-1249 K) is 21.4 grams per kilogram aluminum produced,[14] which agrees well with a value predicted by Solntsev's equation[3] of 21 grams for a cryolite ratio of 2.8 and a temperature of 1248 K. Nineteen percent of this value is 4.1 g. fluoride per kg. aluminum which is taken as a constant for the range of cell parameters treated by the model.

An alternative value can be derived using the estimation of entrainment from measurements of fume calcium content. If entrainment is estimated as 7 percent of overall evolution[8] this gives a value for the entrainment contribution of 1.5 g. fluoride per kg. aluminum produced.

HF Generation

Three possible mechanisms for HF generation are employed in the model, either separately or in some combination. These mechanisms are: generation by hydrolysis of water from the potroom atmosphere, hydrolysis of water contained in the alumina feed to the cell, and reaction with hydrogen-containing impurities within the cell anodes which are released as the anodes are consumed.

HF generation from reaction with potroom humidity is treated by considering the thermodynamics of possible fume-generating reactions between water and bath constituents. Table 3 lists the reactions

between water and the major constituents of the bath and the equilibrium constants of these reactions at 1250 K. Reactions to produce fluorine gas are also thermodynamically possible but were not included as their equilibrium constants are very low (less than 10^{-15} at 1250 K[25]).

TABLE 3

Fume Generating Reactions and Equilibrium Constants at 1250 K[25]

	Reaction	$K_{1250\ K}$
I	$2\ NaF(\ell) + 2\ H_2O(g) = 2\ NaOH(\ell) + 2\ HF(g)$	2.4×10^{-8}
II	$2/3\ Na_3AlF_6(\ell) + H_2O(g) = 1/3\ Al_2O_3(s) + 2\ NaF(\ell) + 2\ HF(g)$	2.7×10^{-3}
III	$2/3\ AlF_3(s) + H_2O(g) = 1/3\ Al_2O_3(s) + 2\ HF(g)$	3.5

In view of the large value for the equilibrium constant for Equation III, and the fact that cryolite baths are generally operated with an excess of aluminum fluoride,[6] it seems reasonable to use this reaction as a basis for calculating the equilibrium partial pressure of HF.

First, the standard Gibbs free energy expression for the reaction as a function of temperature is calculated from thermodynamic data.[26] This gives the following expression:

$$\Delta G^{o}_{III}\ (\text{Joules}) = 130{,}130 - 14.38\ T \log_{10} T - 87.89\ T + 3.27 \times 10^{-3}\ T^2 + 1.7 \times 10^{5}/T$$

writing the expression for the equilibrium constant yields:

$$K_{III} = e^{(-\Delta G^{o}/RT)} = \frac{(a_{Al_2O_3})^{1/3}\ (P_{HF})^2}{(P_{H_2O})\ (a_{AlF_3})^{2/3}}$$

solving for partial pressure of HF, and rewriting with FORTRAN variable names gives:

$$PHF^2 = \frac{(AALF3)^{2/3}\ (PH2O)}{(AAL2O3)^{1/3}}\ e^{(-DGHYD/RT)}$$

PH2O is obtained by dividing the atmospheric humidity by atmospheric pressure, 101325 Pa. (1 atm.). The activity of alumina is obtained by curve fitting data from Vetyukov and Van Ban[27] which gives the equation:

$$AAL2O3 = -3.4218 \times 10^{-4}\ (NAL2O3)^3 + 0.013506\ (NAL2O3)^2$$

$$-0.031509\ (NAL2O3) + 6.1619 \times 10^{-3}\ (-2.0\ CRATIO + 7.0)$$

Similarly, an expression for the activity of AlF_3 is obtained from Sterten and Homberg[28]:

$$\log_{10} AALF3 = 0.2551\ (CRATIO)^2 - 2.105\ (CRATIO) + 0.6625$$

From these relations is obtained the equilibrium partial pressure of HF. This can be converted to fluoride evolution (g. fluorine per kg. aluminum produced) by multiplying by the anode gas evolution rate and the atomic weight of fluorine.

The HF evolution due to anode hydrogen can be treated in two ways. If kinetics are ignored and it is assumed that all hydrogen released by anode consumption subsequently reacts to form HF, then the expression for HF evolution is:

$$WFHF = 18.998\ (ACONS)(HCONTNT)\ \frac{(1000)(2)}{2.016}$$

WFHF is the HF evolution (g. fluorine per kg. aluminum produced) 18.998 is the atomic weight of fluorine, ACONS is anode consumption (kg. carbon per kg. aluminum produced), the factor 2 is

for the moles of HF generated per mole hydrogen gas, and 2.016 is the molecular weight of hydrogen.

The second approach is to use Henry's data[14] to try to estimate any kinetic effects that may alter the above calculations. These data are reproduced below:

TABLE 4

HF Evolution as a Function of Anode Hydrogen Content

Anode Hydrogen Content (wt%)	HF Evolution (g./kg.Al) Actual	Theoretical
0.01	1.7	0.7
0.07	3.4	5.0

From these data it is estimated that an increase of hydrogen content by 0.06 percent actually increased HF evolution by 1.7 grams per kilogram aluminum produced whereas the theoretical increase would be 4.3 grams per kilogram. This gives a factor of 0.4 of the theoretical actually taking place. This factor is then included in the expression previously derived for anode hydrogen.

The final mechanism to consider is the evolution of HF due to moisture in the alumina feed. In this model two different possibilities are considered to account for the fact that it does not appear that all of the water present in the alumina when charged reacts to form HF immediately. The first is that the alumina dries out to approximately 0.1 weight percent water before entering the cell. The second is that due to reaction kinetics not presently understood only 5 percent of the water in the alumina reacts. This is handled in the model by setting WCAD, the water content of alumina entering

the bath, at a maximum of 0.1 for the first case, and multiplying the water content of charged alumina, WCA, by 0.05 to get WCAD for the second case.

In either case, the fluoride evolution due to water in alumina is then calculated as follows:

$$WFHF = 18.998 \times \left(\frac{1888.89\ WCAD}{(18.015)(100)}\right) \times 2$$

where WFHF is the fluoride evolution in grams fluorine per kilogram aluminum, 18.998 is the atomic weight of fluorine, 1888.89 is the alumina consumption in grams alumina per kilogram aluminum produced, 18.015 is the molecular weight of water, and 100 is the conversion factor to convert WCAD from weight percent to weight fraction.

Subroutine FLØRIDE can then be run with any combination of the fluoride evolution mechanisms that have been discussed in this section added together to give total fluoride evolution, which can then be compared to experimental results or empirical expressions. These runs were made using the following range of values of cell parameters. The second value given is the value used when the parameter is held constant.

Temperature - 1210 to 1260 K; 1240 K.

Cryolite Ratio - 2.4 to 2.9; 2.6.

Water Content of Alumina - 0.1 to 2.0 wt%; 2.0 wt%.

Anode Hydrogen Content - 0.0001 to 0.001 g. hydrogen/g. anode.
0.007 g. hydrogen/g. anode

Atmospheric Humidity - 300 to 1700 Pa; 1300 Pa

Alumina Content - 2.0 to 7.0 wt%; 5.0 wt%

CaF_2 Content - 5.0 to 9.0 wt%; 6.0 wt%

The results of these runs are given and discussed in the next section of this report.

Results and Discussion

Standard Model

Upon running the fluoride model it was decided that it would be necessary to have a standard set of the various treatments of fluoride evolution mechanisms discussed in the Procedure. Then each option could be brought in individually and its effect noted.

The choice was made to use those mechanisms that were most proven or were the simplest in the standard. These included the following:

Less and Waddington's figure for percent fluoride due to entrainment.

Alumina dries to a constant 0.1 weight percent on top of cell as hypothesized by Grjotheim.

All of the hydrogen present in the anodes reacts as the anode is consumed to form water (no kinetic factor).

Atmospheric moisture is not a significant factor in hydrogen fluoride evolution.

Use of the data of Kuxmann and Tillessen for vapor pressure above cryolite melts.

The standard model was run varying temperature (1210 to 1260 K), cryolite ratio (2.4 to 2.9), and anode hydrogen content (0.0001 to 0.001 weight fraction of hydrogen). The other variables were set at the values given in the Procedure.

Table 5 and Figure 1 show the effect of varying bath temperature. The model calculations are compared against the correlations of Alcoa (Haupin), Henry, and Solntsev. Considering the broad range of data

TABLE 5

Fluoride Evolution as a Function of Bath Temperature for the Standard Model

Assumptions for this Table and Figure 1 following:

Bath vapor pressure data of Kuxmann and Tillessen
Entrainment figure of Less and Waddington
Constant water content of alumina of 0.1 wt%
No kinetic factor for anode hydrogen reaction
No HF generation due to potroom humidity

Temperature (°K)	Fluoride Evolution (g. fluorine/kg. aluminum produced)						
	Calculated by Model				Experimental Correlations		
	Vaporization	Entrainment	HF	Total	Solntsev	Alcoa	Henry
1210	4.62	3.4	9.31	17.33	24.31	8.29	14.12
1220	5.38	"	9.29	18.07	24.78	10.73	17.20
1230	6.25	"	9.26	18.91	25.25	13.17	20.49
1240	7.24	"	9.24	19.88	25.72	15.61	23.96
1250	8.37	"	9.21	20.98	26.19	18.05	27.62
1260	9.65	"	9.19	22.24	26.66	20.49	31.44

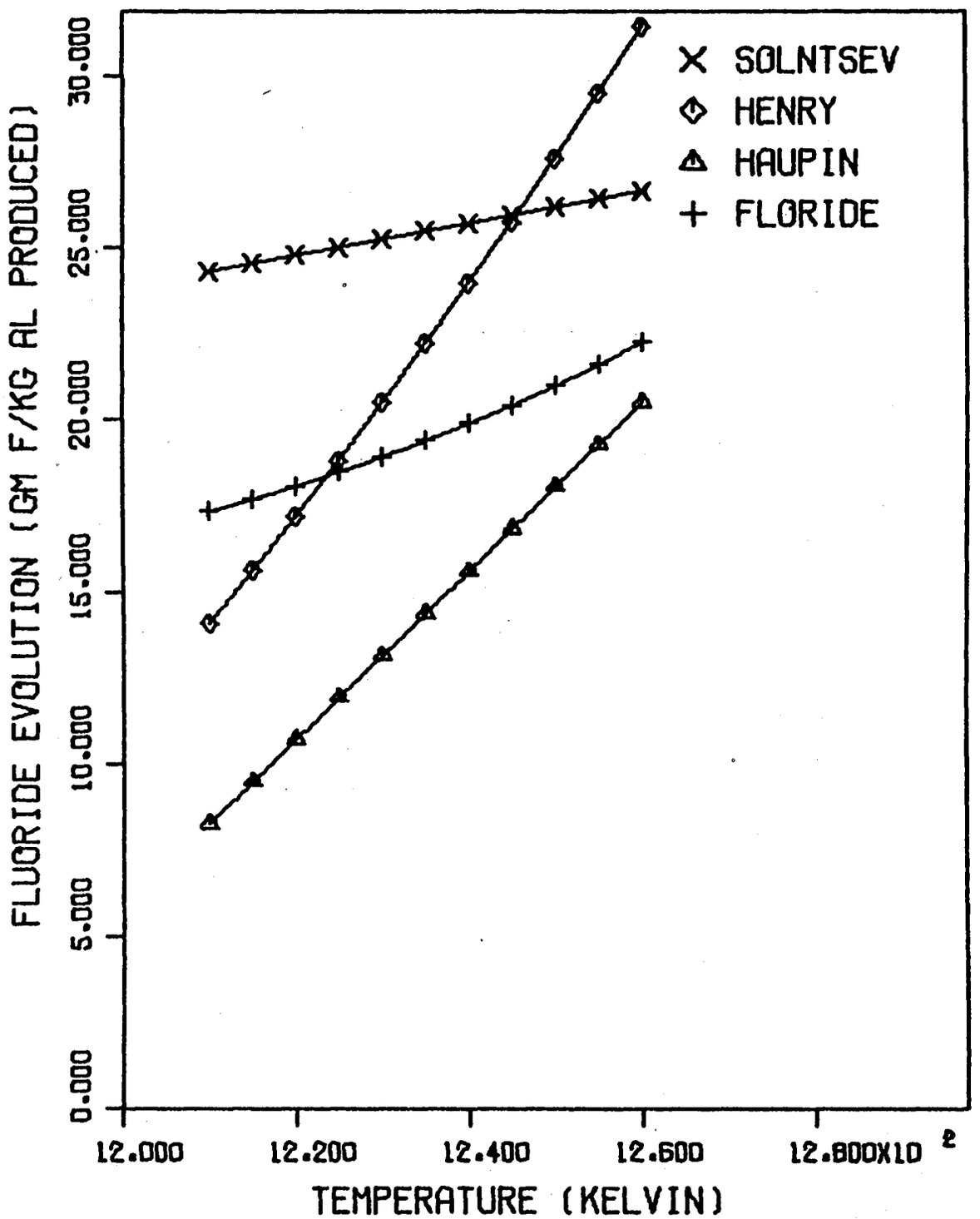

Figure 1

Fluoride Evolution as a Function of Temperature

Standard Model

Refer to Table 5 for assumptions used.

covered by the correlations, the model calculations appear to agree well as they fall well into the middle of the range. In addition, the trend (slope of the line) of the model agrees well with the Solntsev line and fairly well with Haupin's line. It can be concluded that the standard model effectively predicts the effect of bath temperature over the range considered.

The effect of varying cryolite ratio is shown in Table 6 and Figure 2, again comparing the model predictions with the curves of Haupin, Henry, and Solntsev. Again, the model curve falls within the range of the experimental correlations. The trend of the model results do not agree as well this time with the correlations, especially with that of Henry. This is especially significant since the trends of the three correlations are in agreement. The conclusion is that the standard model is only fair at predicting the effect of changes in cryolite ratio.

The effect of varying anode hydrogen content is given on pages 56 through 59, along with the results for the modified version of the model using a kinetic factor for anode hydrogen. Discussion of these data is included with the discussion of the anode hydrogen mechanism later in this section.

Vaporization Options

The only variation considered on the vaporization mechanism was the substitution of an expression to calculate vapor pressure of $NaAlF_4$ using the data of Vajna and Bacchiega[24] rather than that of Kuxmann and Tillessen.[19] As stated in the Procedure, the purpose of this change is to investigate the variation of fluoride evolution with

TABLE 6

Fluoride Evolution vs. Cryolite Ratio for the Standard Model

Assumptions for this Table and Figure 2 following:

Bath vapor pressure data of Kuxmann and Tillessen
Entrainment figure of Less and Waddington
Constant water content of alumina of 0.1 wt%
No kinetic factor for anode hydrogen reaction
No HF generation due to potroom humidity

Cryolite Ratio (moles NaF/moles AlF_3)	Fluoride Evolution (g. fluorine/kg. aluminum produced)						
	Calculated by Model				Experimental Correlations		
	Vaporization	Entrainment	HF	Total	Solntsev	Alcoa	Henry
2.4	9.44	3.4	9.18	22.01	32.89	21.01	27.56
2.5	8.26	"	9.21	20.87	29.09	18.31	25.91
2.6	7.24	"	9.24	19.88	25.72	15.61	23.96
2.7	6.35	"	9.27	19.02	22.72	12.91	21.70
2.8	5.57	"	9.29	18.27	20.04	10.21	19.12
2.9	4.90	"	9.32	17.62	17.62	7.51	16.23

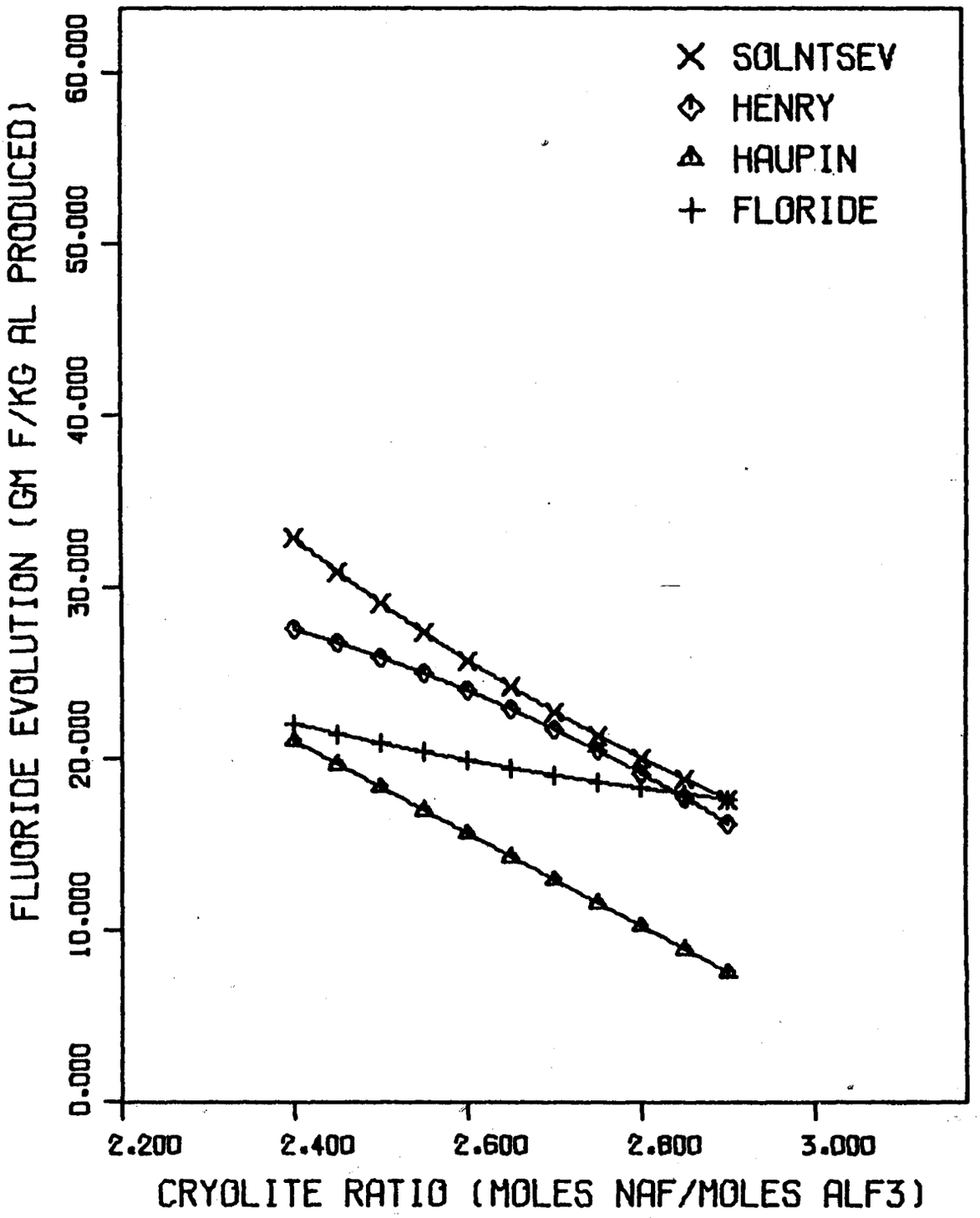

Figure 2

Fluoride Evolution as a Function of Cryolite Ratio

Standard Model

Refer to Table 6 for assumptions used.

alumina and calcium fluoride content and to compare the effects of two differing sets of vapor pressure data.

Using this variation, fluoride evolution was calculated as a function of temperature, cryolite ratio, alumina content, and calcium fluoride content. The results of varying temperature are shown in Table 7 and Figure 3 along with the regression curves from the data of Solntsev, Henry, and Haupin of Alcoa. It can be seen that the model calculations in this case fall at the lower end of the range predicted by the correlations. Only Haupin's data falls within the same range. The trend of the model curve agrees with Solntsev's data but not with the other two curves. In contrast the standard model (Figure 1) fits in the middle of the range of data, and its slope is closer to the average of the three curves. From these observations it can be concluded that use of Vajna and Bacchiega's data results in a poorer prediction of the effect of varying bath temperature.

For cryolite ratio (Table 8 and Figure 4) the results are similar. The model curve predicts a lower range of values and a much different slope which does not correlate as well with the data curves as the standard model (Figure 2). Again it can be concluded that use of Vajna and Bacchiega's vapor pressure values do not produce as good a correlation as using the data of Kuxmann and Tillessen when cryolite ratio is varied. Fluoride evolution as a function of alumina content for the option using Vajna and Bacchiega's data is shown in Table 9 and Figure 5. The correlations of Henry and Haupin are included for comparison. The model prediction falls within the range of Haupin's

TABLE 7

Fluoride Evolution vs. Temperature, Using Vapor Pressure Data of Vajna and Bacchiega

Assumptions for this Table and Figure 3 following:

Bath vapor pressure data of Vajna and Bacchiega
Entrainment figure of Less and Waddington
Constant water content of alumina of 0.1 wt%
No kinetic factor for anode hydrogen reaction
No HF generation due to potroom humidity

Temperature (°K)	Fluoride Evolution (g. fluorine/kg. aluminum produced)						
	Calculated by Model				Experimental Correlations		
	Vaporization	Entrainment	HF	Total	Solntsev	Alcoa	Henry
1210	1.53	3.4	9.31	14.25	24.31	8.29	14.12
1220	1.82	3.4	9.29	14.50	24.78	10.73	17.20
1230	2.15	3.4	9.26	14.81	25.25	13.17	20.49
1240	2.53	3.4	9.24	15.16	25.72	15.61	23.96
1250	2.97	3.4	9.21	15.58	26.19	18.05	27.62
1260	3.48	3.4	9.19	16.06	26.66	20.49	31.44

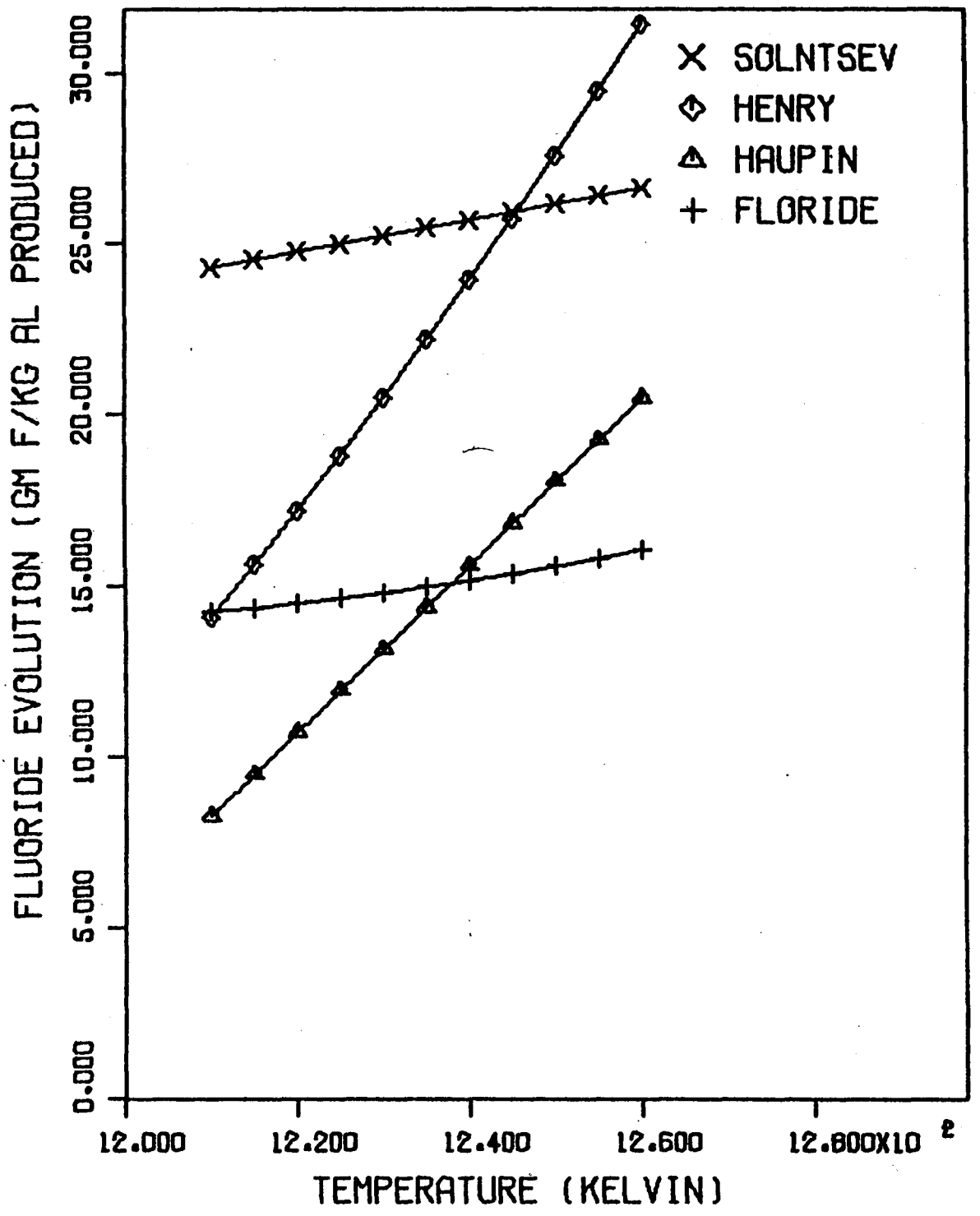

Figure 3

Fluoride Evolution as a Function of Temperature

Using Vapor Pressure Data of Vajna and Bacchiega

Refer to Table 7 for assumptions used.

TABLE 8

Fluoride Evolution vs. Cryolite Ratio Using Vapor Pressure Data of Vajna and Bacchiega

Assumptions for this Table and for Figure 4 following:

Bath vapor pressure data of Vajna and Bacchiega
Entrainment figure of Less and Waddington
Constant water content of alumina of 0.1 wt%
No kinetic factor for anode hydrogen reaction
No HF generation due to potroom humidity

Cryolite Ratio (moles NaF/Moles $A\ell F_3$)	Fluoride Evolution (g. fluorine/kg. aluminum produced)						
	Calculated by Model				Experimental Correlations		
	Vaporization	Entrainment	HF	Total	Solntsev	Alcoa	Henry
2.4	2.99	3.4	9.18	15.57	32.89	21.01	27.56
2.5	2.75	"	9.21	15.35	29.09	18.31	25.91
2.6	2.53	"	9.24	15.16	25.72	15.61	23.96
2.7	2.32	"	9.27	14.99	22.72	12.91	21.70
2.8	2.14	"	9.29	14.83	20.04	10.21	19.12
2.9	1.97	"	9.32	14.69	17.62	7.51	16.23

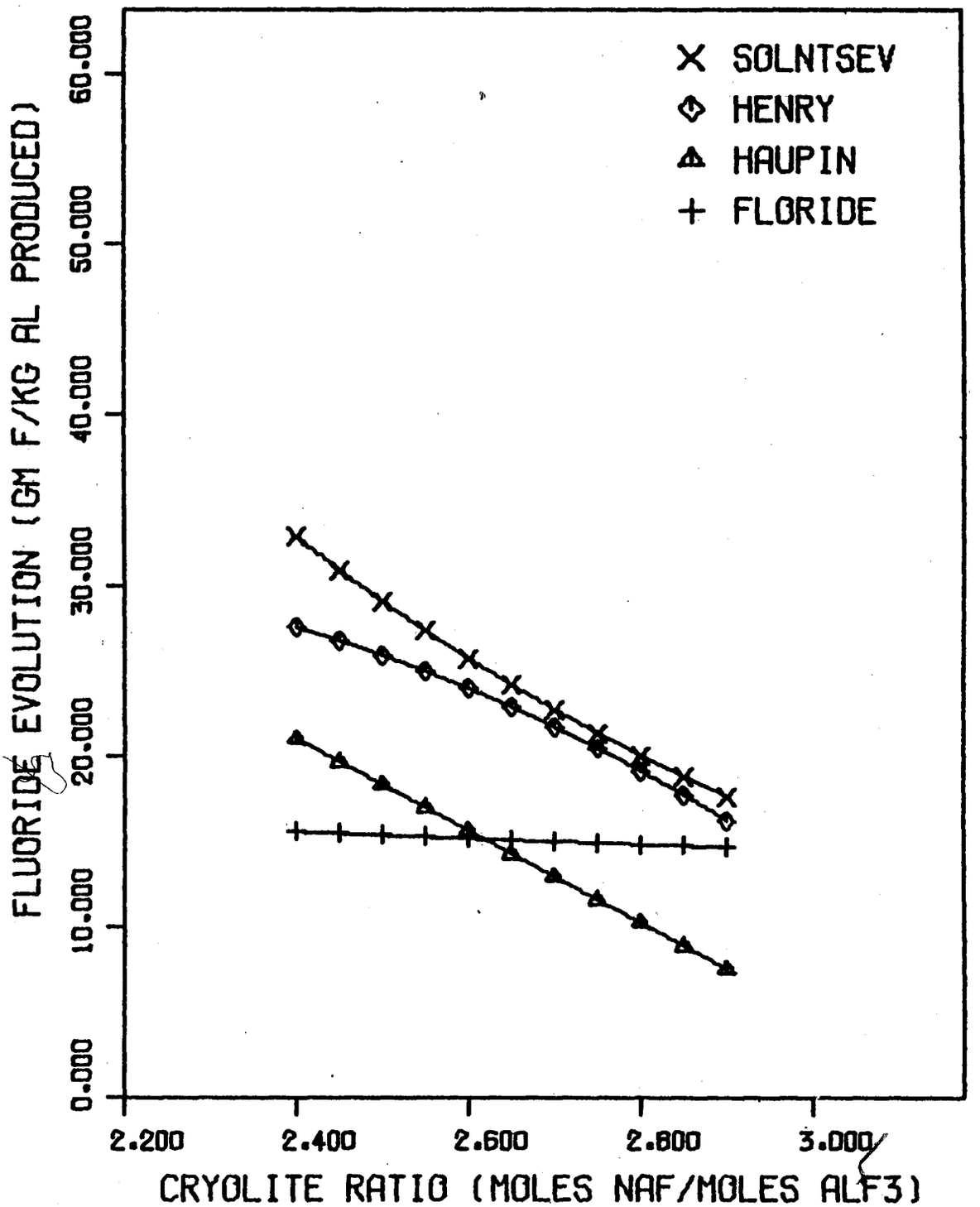

Figure 4

Fluoride Evolution as a Function of Cryolite Ratio
Using Vapor Pressure Data of Vajna and Bacchiega
Refer to Table 8 for the assumptions used.

TABLE 9

Fluoride Evolution vs. Weight Percent Alumina using Vapor Pressure Data of Vajna and Bacchiega

Assumptions for this Table and for Figure 5 following:

Bath vapor pressure data of Vajna and Bacchiega
Entrainment figure of Less and Waddington
Constant water content of alumina of 0.1 wt%
No kinetic factor for anode hydrogen reaction
No HF generation due to potroom humidity

Alumina in Bath Weight Percent	Fluoride Evolution (g. fluorine/kg. aluminum produced)					
	Calculated by Model				Experimental Correlations	
	Vaporization	Entrainment	HF	Total	Alcoa	Henry
2.0	3.19	3.4	9.17	15.77	19.48	30.57
3.0	2.95	"	9.19	15.55	18.19	28.38
4.0	2.73	"	9.22	15.35	16.90	26.18
5.0	2.53	"	9.24	15.16	15.61	23.96
6.0	2.34	"	9.26	14.99	14.32	21.72
7.0	2.16	"	9.28	14.84	13.03	19.46

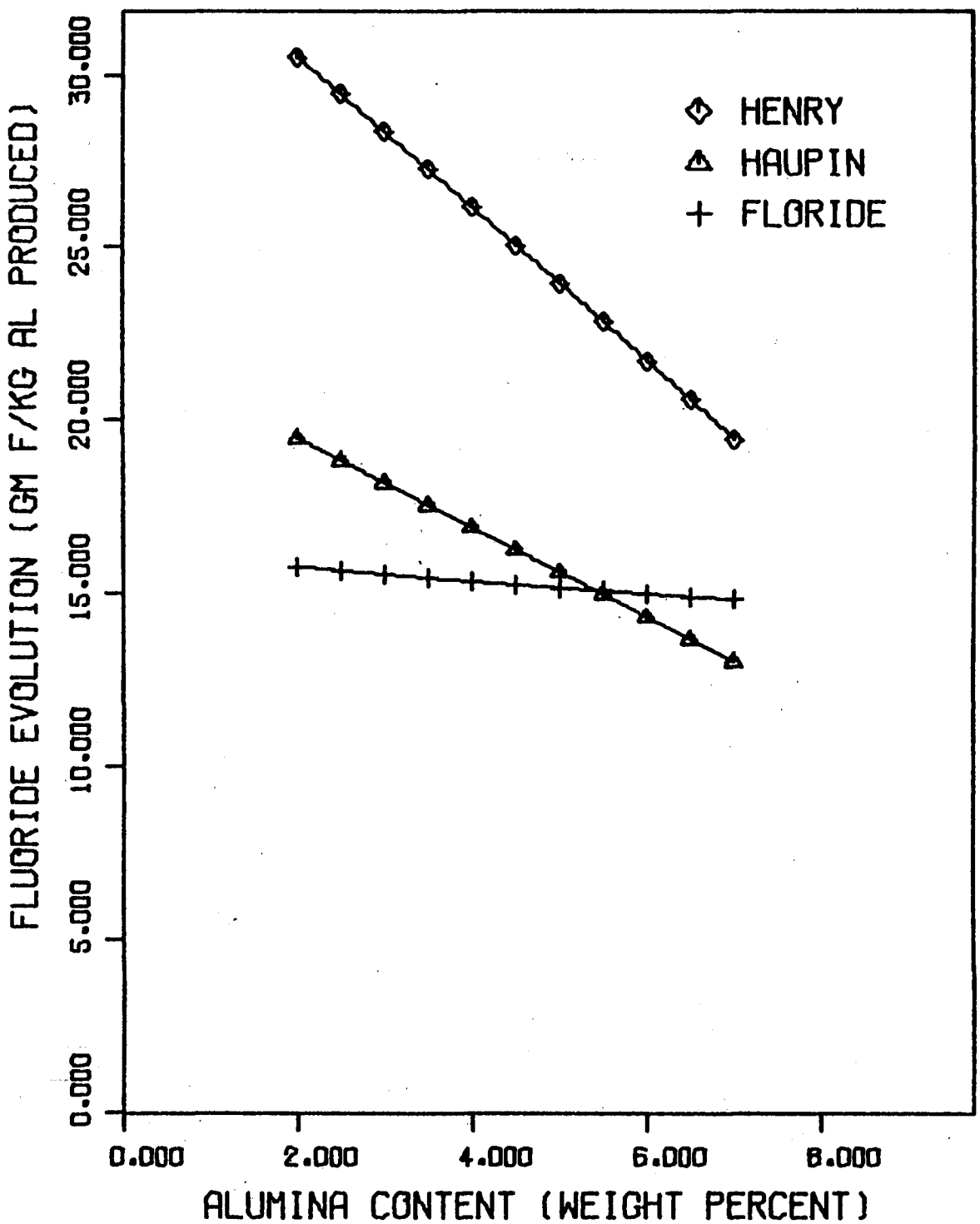

Figure 5

Fluoride Evolution as a Function of Bath Alumina Content

Using Vapor Pressure Data of Vajna and Bacchiega

Refer to Table 9 for assumptions used.

data but well below that of Henry. The rate of change of the model curve is much less than that of either experimental correlation. From this it can be concluded that the model using Vajna and Bacchiega's data is only fair at best in predicting the effect of varying alumina content.

In Table 10 the effect of varying calcium fluoride content is shown. In this case no experimental data are available for comparison so no conclusions can be drawn as to the effectiveness of the model in predicting this behavior, but the model results are included in case these data become available in the future. In any case, it can be observed that the effects of varying CaF_2 appear to be very slight.

In summary, it would appear that the use of Vajna and Bacchiega's vapor pressure data results in a model that predicts the effect of temperature and cryolite ratio less well than using Kuxmann and Tillessen's data, and that gives only a fair prediction of the effect of varying alumina content. In spite of the fact that they lack data on the effect of varying alumina and calcium fluoride content, the results of Kuxmann and Tillessen's work appear to be the optimum of the two sets of vapor pressure data for inclusion in this model.

Entrainment Options

The only variation considered of the entrainment mechanism was the use of a number for fluoride fume entrained based on the percentage reported by Haupin. As previously noted, the standard model used the percentage given by Less and Waddington.

Using this variation, fluoride evolution was calculated as a function of temperature and cryolite ratio. The other cell parameters

TABLE 10

Fluoride Evolution vs Weight Percent Calcium Fluoride using Vapor Pressure Data of Vajna and Bacchiega

Assumptions for this Table:

Bath vapor pressure data of Vajna and Bacchiega
Entrainment figure of Less and Waddington
Constant water content of alumina of 0.1 wt%
No kinetic factor for anode hydrogen reaction
No HF generation due to potroom humidity

CaF_2 in bath Weight Percent	Fluoride Evolution (g. fluorine/kg. aluminum produced) Calculated by Model			
	Vaporization	Entrainment	HF	Total
5.0	2.73	3.4	9.23	15.36
6.0	2.63	"	9.23	15.26
7.0	2.34	"	9.24	14.98
8.0	2.16	"	9.25	14.81
9.0	2.00	"	9.25	14.65

were set at the values given in the Procedure.

The results of the model, along with the curves of Haupin, Henry, and Solntsev, are given in Table 11 and Figure 6. The range of the model predictions appears to be toward the lower end of the range of experimental values. Compared to the values calculated by the standard model (Figure 1) this variation gives results that correlate slightly better with Haupin's data but not as well with the other two curves. The trends in both cases are the same. The results for cryolite ratio (Table 12 and Figure 7) show similar effects, with the model line correlating better with Haupin's regression. In both cases (temperature and cryolite ratio) the difference between the variation using Haupin's figure for entrainment and the standard model is slight reflecting the relatively smaller contribution of entrainment, the fact that entrainment is taken to be constant in this model, and the large variation in experimental results implied by the differences between the correlations used for comparison. Therefore no conclusions can be drawn here as to which figure for entrainment is more effective for use within the model.

HF Generation Options

HF Generation from Potroom Humidity

As noted in the introduction, several workers[2,14,25] have proposed that moisture in the potroom atmosphere could be a significant source of water for HF generation. To test this hypothesis, the model was run with only the atmospheric moisture mechanism operative. Fluoride evolution was determined as a function of temperature, cryolite ratio, and atmospheric humidity. The results of varying tempera-

TABLE 11

Fluoride Evolution vs. Temperature using Entrainment Derived from Haupin's Work

Assumptions for this Table and Figure 6 following:

Bath vapor pressure of Kuxmann and Tillessen
Entrainment figure of Haupin
Constant water content of alumina of 0.1 wt%
No kinetic factor for anode hydrogen reaction
No HF generation due to potroom humidity

Temperature °K	Fluoride Evolution (g. fluorine/kg. aluminum produced)						
	Calculated by Model				Experimental Correlations		
	Vaporization	Entrainment	HF	Total	Solntsev	Haupin	Henry
1210	4.62	1.5	9.31	15.43	24.31	8.29	14.12
1220	5.38	"	9.29	16.17	24.78	10.73	17.20
1230	6.25	"	9.26	17.01	25.25	13.17	20.49
1240	7.24	"	9.24	17.98	25.72	15.61	23.96
1250	8.37	"	9.21	19.08	26.19	18.05	27.62
1260	9.65	"	9.19	20.34	26.66	20.49	31.44

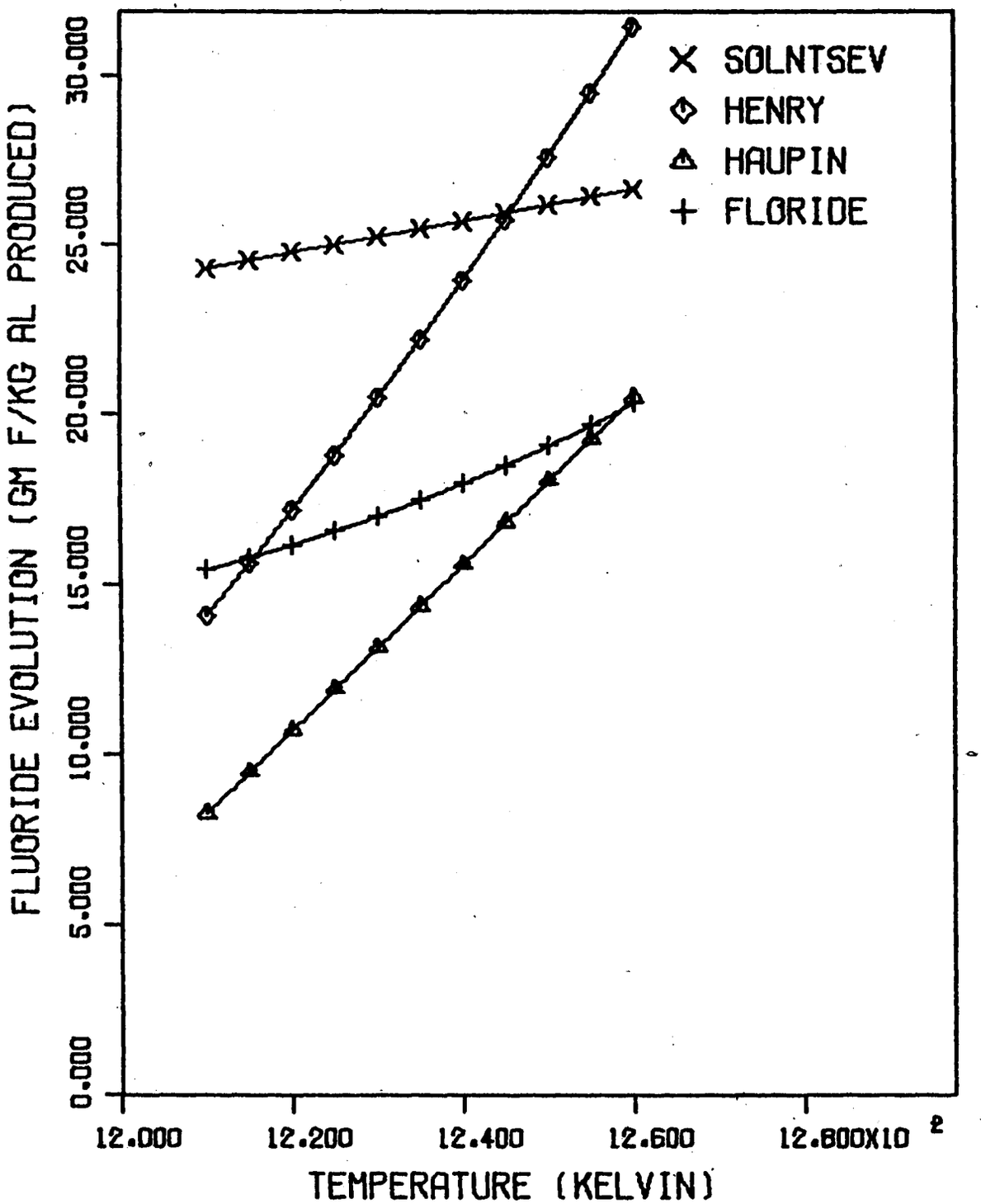

Figure 6

Fluoride Evolution as a Function of Temperature
Using Entrainment Derived from Haupin's Work
Refer to Table 11 for assumptions used.

TABLE 12

Fluoride Evolution vs. Cryolite Ratio Using Entrainment Derived from Haupin's Work

Assumptions for this Table and Figure 7 following:

Bath vapor pressure of Kuxmann and Tillessen
Entrainment figure of Haupin
Constant water content of alumina of 0.1 wt%
No kinetic factor for anode hydrogen reaction
No HF generation due to potroom humidity

Cryolite Ratio (moles NaF/moles AlF_3)	Fluoride Evolution (g. fluorine/kg. aluminum produced)						
	Calculated by Model				Experimental Correlations		
	Vaporization	Entrainment	HF	Total	Solntsev	Haupin	Henry
2.4	9.44	1.5	9.18	20.11	32.89	21.01	27.56
2.5	8.26	"	9.21	18.98	29.09	18.31	25.91
2.6	7.24	"	9.24	17.98	25.72	15.61	23.96
2.7	6.35	"	9.27	17.12	22.72	12.91	21.70
2.8	5.57	"	9.29	16.37	20.04	10.21	19.12
2.9	4.90	"	9.32	15.72	17.62	7.51	16.23

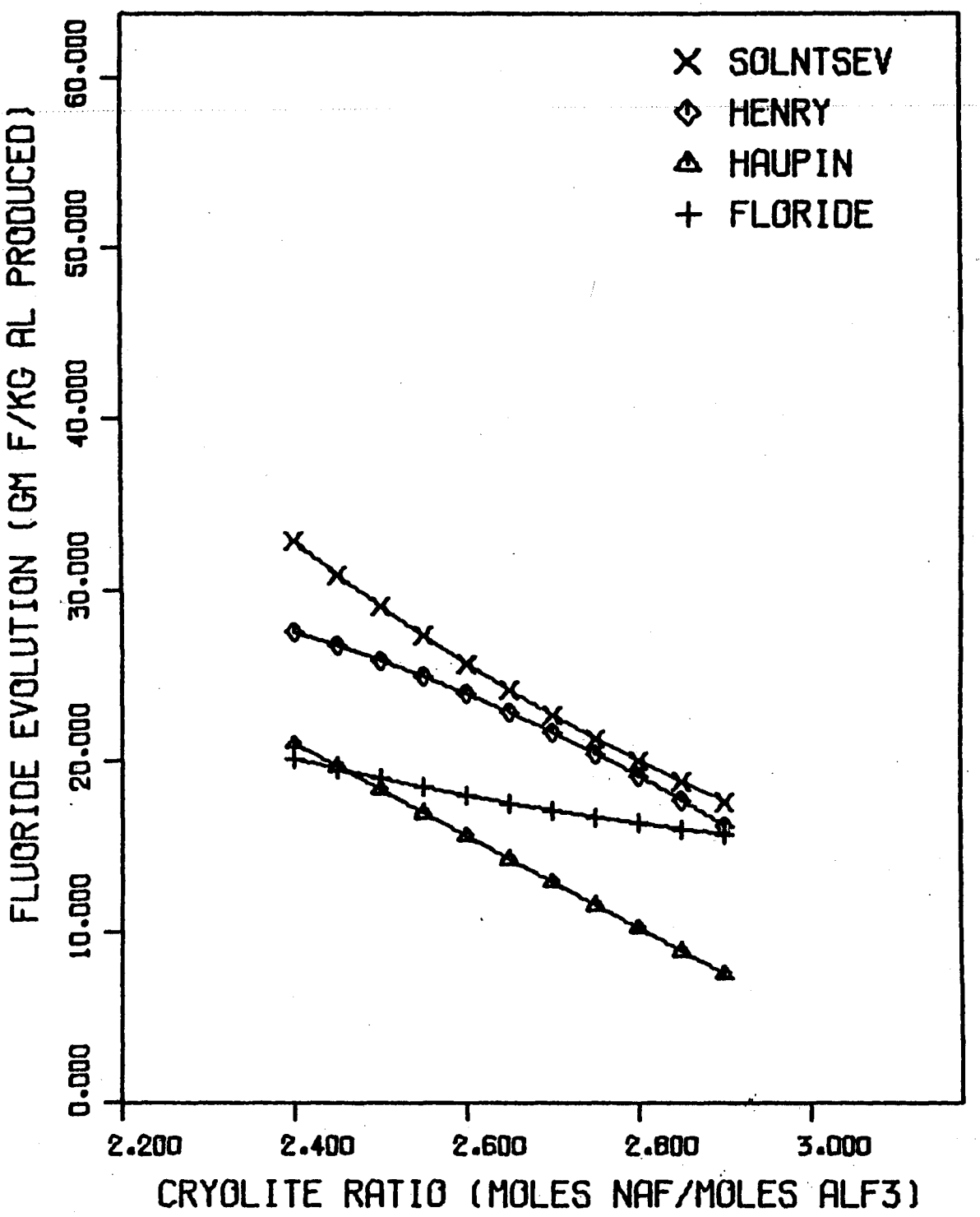

Figure 7

Fluoride Evolution as a Function of Cryolite Ratio
Using Entrainment Derived from Haupin's Work
Refer to Table 12 for the assumptions used.

ture are shown in Table 13 and Figure 8 and the results of varying cryolite ratio are shown in Table 14 and Figure 9. In both cases, the range of values predicted by the model is outside that given by the experimental curves and range from 20 to 100 percent greater. The slopes of the lines correlate well except for Solntsev's line when temperature is varied. It would appear that the model using this mechanism for HF evolution gives good predictions of the trends in total fluoride evolution as a function of bath temperature and cryolite ratio. However, it is not very effective at predicting the value of total fluoride evolution to be expected.

Fluoride evolution as a function of atmospheric humidity was also calculated. These results are shown in Table 15 and Figure 10 along with the calculated values from Haupin's regression equation and some values derived from calculations by Cochran, Sleppy, and Frank.[25] The points labeled Cochran are calculated using their HF data, combined with vaporization and entrainment data from FLORIDE. The fluoride model gives results that considerably exceed the data of Haupin. In addition, the slope of the line is much greater. The model calculations also differ from those derived from Cochran, Sleepy, and Frank. This would seem to indicate that although there is a variation of fluoride evolution with potroom humidity, it is not as significant as this version of the model predicts using the method for calculating HF vapor pressure described in the procedure. If the method described by Cochran, Sleppy, and Frank had been used, the results would undoubtedly be closer to the results of Haupin's regression equation.

TABLE 13

Fluoride Evolution vs. Temperature using Atmospheric Humidity Mechanism

Assumptions for this Table and Figure 8 following:

Bath vapor pressure of Kuxmann and Tillessen
Entrainment figure of Less and Waddington
HF generation from hydrolysis by moisture from potroom atmosphere

Temperature °K	Fluoride Evolution (g. fluorine/kg. aluminum produced)						
	Calculated by Model				Experimental Correlations		
	Vaporization	Entrainment	HF	Total	Solntsev	Haupin	Henry
1210	4.62	3.4	20.29	28.31	24.31	8.29	14.12
1220	5.38	"	21.28	30.07	24.78	10.73	17.20
1230	6.25	"	22.31	31.96	25.25	13.17	20.49
1240	7.24	"	23.36	34.00	25.72	15.61	23.96
1250	8.37	"	24.44	36.21	26.19	18.05	27.62
1260	9.65	"	25.55	38.60	26.66	20.49	31.44

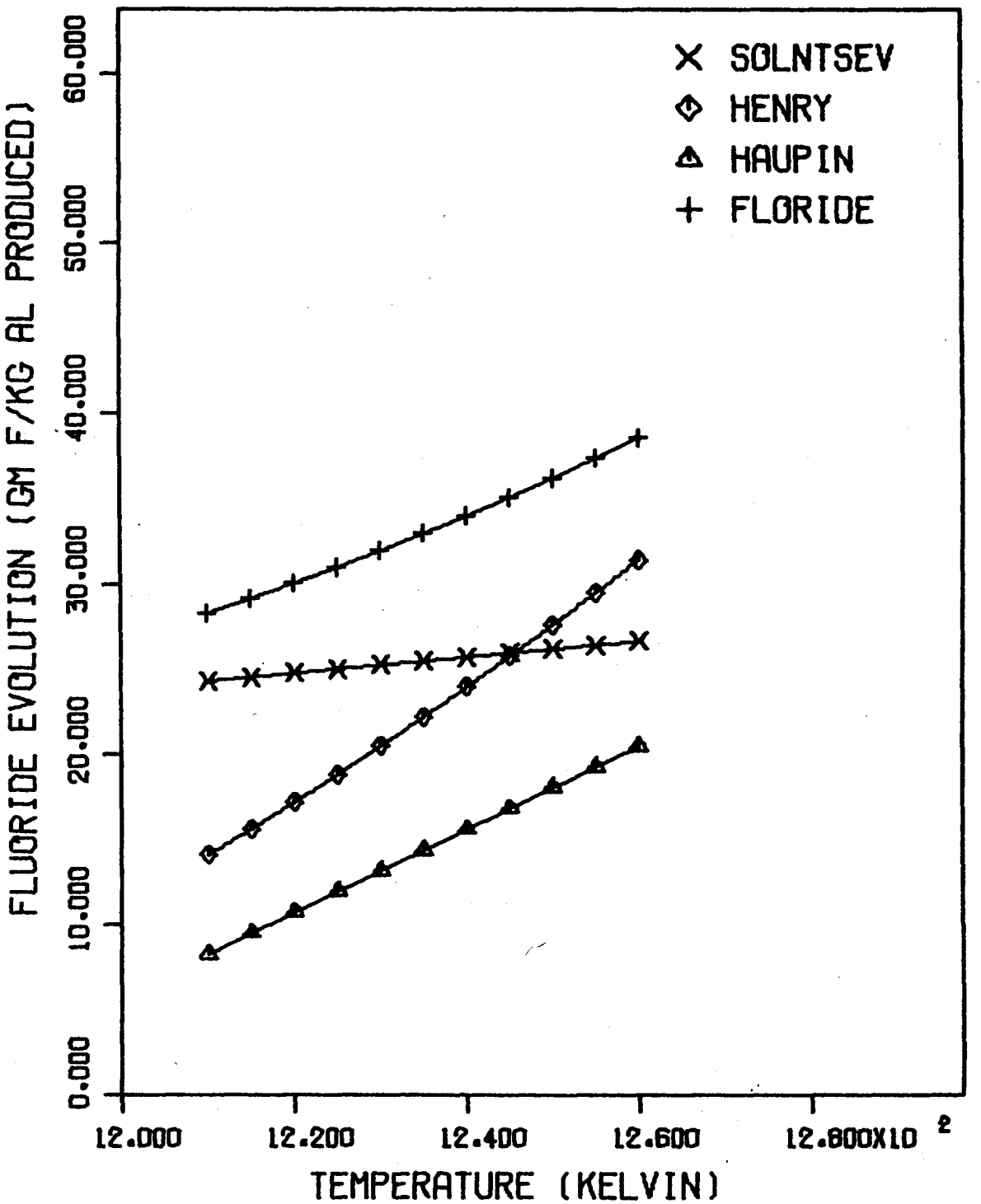

Figure 8

Fluoride Evolution as a Function of Temperature

Using Atmospheric Humidity Mechanism

Refer to Table 13 for assumptions used.

TABLE 14

Fluoride Evolution vs. Cryolite Ratio using Atmospheric Humidity Mechanism

Assumptions for this Table and Figure 9 following:

Bath vapor pressure of Kuxmann and Tillessen
Entrainment figure of Less and Waddington
HF generation from hydrolysis by moisture from potroom atmosphere

Cryolite Ratio (moles NaF/moles $A\ell F_3$)	Fluoride Evolution (g. fluorine/kg. aluminum produced)						
	Calculated by Model				Experimental Correlations		
	Vaporization	Entrainment	HF	Total	Solntsev	Haupin	Henry
2.4	9.44	3.4	25.37	38.21	32.89	21.01	27.56
2.5	8.26	"	24.28	35.94	29.09	18.31	25.91
2.6	7.24	"	23.36	34.00	25.72	15.61	23.96
2.7	6.35	"	22.61	32.36	22.72	12.91	21.70
2.8	5.57	"	22.02	31.00	20.04	10.21	19.12
2.9	4.90	"	21.61	29.90	17.62	7.51	16.23

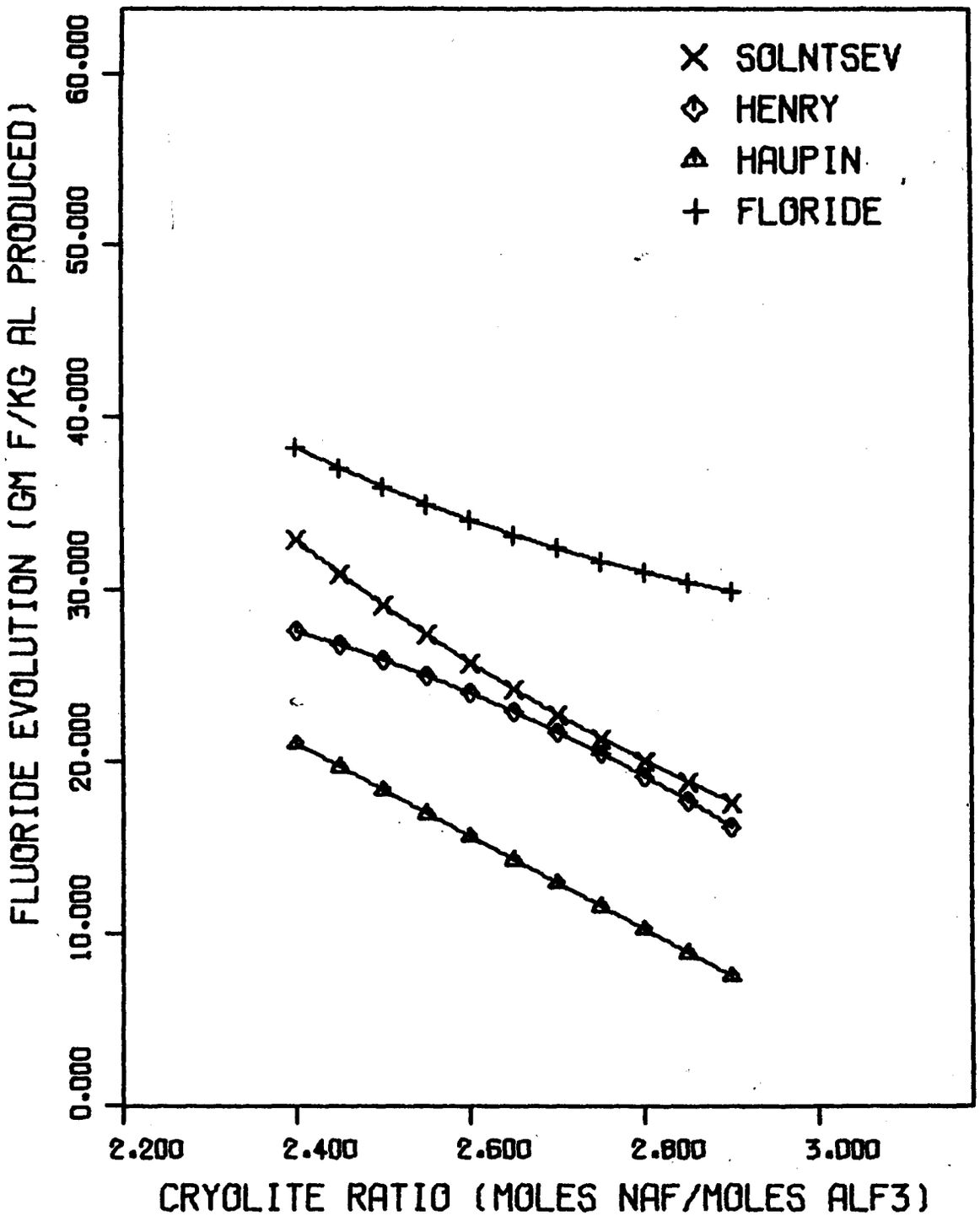

Figure 9

Fluoride Evolution as a Function of Cryolite Ratio
Using Atmospheric Humidity Mechanism
Refer to Table 14 for assumptions used.

TABLE 15

Fluoride Evolution vs. Humidity using Atmospheric Humidity Mechanism

Assumptions for this Table and Figure 10 following:

Bath vapor pressure of Kuxmann and Tillessen
Entrainment figure of Less and Waddington
HF generation from hydrolysis by moisture from potroom atmosphere

Atmospheric Humidity (Pascals)	Fluoride Evolution (g. fluorine/kg. aluminum produced)				
	Calculated by Model				Experimental Correlation
	Vaporization	Entrainment	HF	Total	Haupin
300	7.24	3.4	11.22	21.86	11.84
500	"	"	14.49	25.13	12.60
700	"	"	17.14	27.18	13.35
900	"	"	19.43	30.08	14.10
1100	"	"	21.49	32.13	14.86
1300	"	"	23.36	34.00	15.61
1500	"	"	25.09	35.73	16.37
1700	"	"	26.71	37.35	17.12

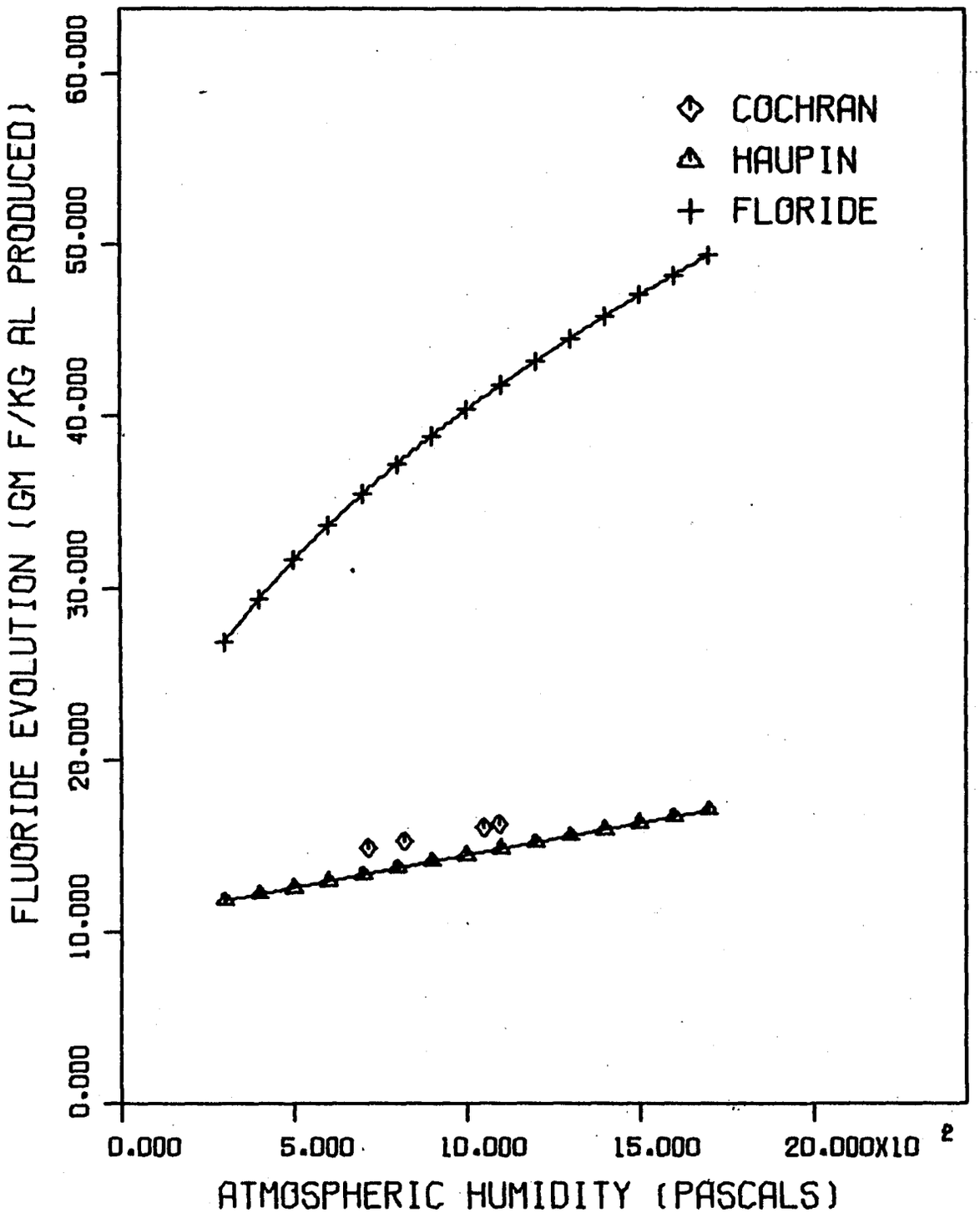

Figure 10

Fluoride Evolution as a Function of Atmospheric Humidity

Using Atmospheric Humidity Mechanism

Refer to Table 15 for assumptions used.

The reason for the different results appears to be due to use of different reaction equations and thermodynamic data. Although it would seem at first that calculations, even though based on different reaction equilibria, should yield similar results, it should be considered that small differences in thermodynamic data can cause differences of an order of magnitude or more in the calculated partial pressures. This is due to the fact that the equilibrium constant is an exponential function of free energy. For example the Gibbs free energy at 1250 K for the reaction:

$$\frac{2}{3}\,Al F_3(s) + H_2O(g) = \frac{1}{3}\,Al_2O_3(s) + 2\,HF(g)$$

is calculated as -7046 cal./mole using the data of Kubaschewski, Evans, and Alcock[26] (as used in the fluoride model) while values interpolated from JANAF tables[29] give a value of -12,328 cal./mole. This yields equilibrium constants of 17.1 and 143.1 respectively. Cochran, Sleppy, and Frank list a value of 3.5 calculated from the then current (1970) JANAF tables. It turns out that these differences are reasonable when the experimental error in the free energy values are considered. Therefore a difference of an order of magnitude can exist in the partial pressure of HF value, the error depending upon the thermochemical data used. Unfortunately, Cochran, Sleppy, and Frank do not list the source of their data, including the activity data for Al_2O_3 and $NaAlF_4$, which they use to derive their values of HF partial pressure. If these sources were available, the differences could be further pinpointed.

In summary, use of the potroom moisture mechanism of HF evolution as the sole HF generation mechanism as included in FLORIDE appears to be effective only in predicting trends in total fluoride evolution as a function of temperature and cryolite ratio. The model using this variation predicts total fluoride values that are much too high.

HF Generation from Anode Hydrogen

The mechanism for HF evolution through hydrolysis by water from anode hydrogen can be treated either by only considering the release rate of hydrogen from the anodes or optimally considering a kinetic factor attributable to some rate controlling step within the subsequent reactions. Fluoride evolution as a function of anode hydrogen content is presented in Table 16 using the former treatment and Table 17 using the latter treatment with kinetic factor. Both results are included in Figure 11 along with the experimental regression line of Haupin. The results show that the model version with kinetic factor is much more effective at predicting the effect of varying hydrogen content. The increase in evolution with increasing hydrogen content exceeds slightly that shown by Haupin's curve, indicating that the kinetic factor is slightly lower than 0.4. However, the data certainly justifies a consideration of kinetics instead of the assumption that no kinetic factor exists.

HF Generation from Alumina Moisture

To examine the hypothesis that there is a significant variation of HF evolution with alumina water content, fluoride evolution was calculated as a function of alumina water content using the model

TABLE 16

Fluoride Evolution vs. Anode Hydrogen Content for the Standard Model

Assumptions for this Table and curve labelled Standard in Figure 11 following:

Bath vapor pressure of Kuxmann and Tillessen
Entrainment figure of Less and Waddington
No HF generation from potroom atmospheric moisture
Constant 0.1 wt% of water in alumina reactions
All anode hydrogen released reacts to form HF (no kinetic factor)

Anode Hydrogen Content (g. hydrogen/g. anode)	Fluoride Evolution (g. fluorine/kg. aluminum produced)				
	Calculated by Model				Experimental Correlation
	Vaporization	Entrainment	HF	Total	Haupin
.0001	7.24	3.4	4.73	15.38	15.04
.0003	"	"	6.24	16.88	15.23
.0005	"	"	7.74	18.38	15.42
.0007	"	"	9.24	19.88	15.61
.0009	"	"	10.74	21.38	15.80
.001	"	"	11.49	22.13	15.90

TABLE 17

Fluoride Evolution vs. Anode Hydrogen Content using Kinetic Factor for Anode Hydrogen Reaction

Assumptions for this Table and curve labelled Kinetic Factor in Figure 11 following:

Bath vapor pressure of Kuxmann and Tillessen
Entrainment figure of Less and Waddington
No HF generation from potroom atmospheric moisture
Constant 0.1 wt% of water in alumina reaction
Only 40% of anode hydrogen available reacts to form HF

Anode Hydrogen Content (g. hydrogen/g. anode)	Fluoride Evolution (g. fluorine/kg. aluminum produced)				
	Calculated by Model				Experimental Correlation
	Vaporization	Entrainment	HF	Total	Haupin
.0001	7.24	3.4	4.28	14.93	15.04
.0003	"	"	4.88	15.53	15.23
.0005	"	"	5.49	16.13	15.42
.0007	"	"	6.09	16.73	15.61
.0009	"	"	6.69	17.33	15.80
.001	"	"	6.99	17.63	15.90

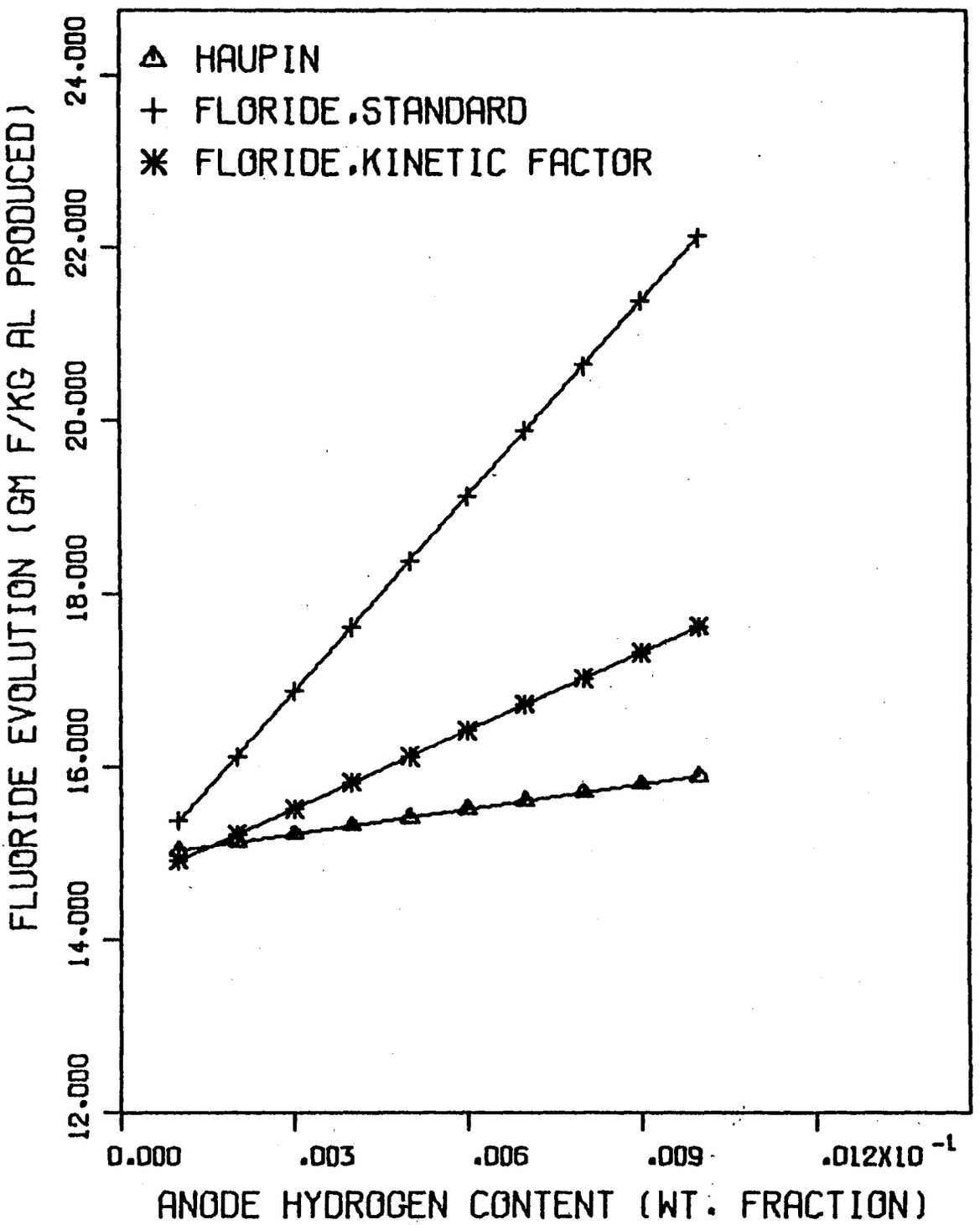

Figure 11

Fluoride Evolution as a Function of Anode Hydrogen Content

Figure includes the standard model and the option using a kinetic factor for the anode hydrogen reaction.

Refer to Tables 16 and 17 for the assumptions used.

and the regression equations of Henry and Haupin. The results are shown in Table 18 and Figure 12. For comparison, it might be noted that the standard model, assuming a constant reaction to the extent of 0.1 weight percent no matter what the water content, would give a figure for total fluoride evolution of 20 grams/kilogram aluminum produced.

The model correlates well with the experimental curve of Henry. This is as expected, since these data were the source of the 5 percent factor. However, the model also correlates well with Haupin's curve, especially with regard to trend. This is not conclusive proof since it is possible that there is enough scatter in the data Haupin used to justify even the assumption of a constant value of 0.1 weight percent for alumina moisture. Even so, the fact that a correlation of some sort does exist which nearly matches the assumption of 5% moisture reacting does tend to support this hypothesis.

This does seem reasonable when the moisture loss of alumina upon heating is considered. Normal temperature on the cell crust for a prebake cell is 703 - 823 K.[14] In this temperature range Henry estimates that alumina (normally about 2% water as received) would dry to 0.2 to 0.5% water. These values agree with water contents calculated from Cochran, Sleppy and Frank's[25] data on weight loss of alumina recovered from cell fumes, after correction for HF loss. These data are reproduced in Table 19 .

TABLE 18

Fluoride Evolution vs. Alumina Water Content using Assumption that 5 Percent of Alumina Moisture Reacts.

Assumptions for this Table and Figure 12 following:

Bath vapor pressure of Kuxmann and Tillessen
Entrainment figure of Less and Waddington
No HF generation from potroom atmospheric moisture
Water in alumina feed reacts to the extent of 5% to form HF
All anode hydrogen released reacts to form HF (no kinetic factor)

Alumina Water Content (wt.%)	Fluoride Evolution (g. fluorine/kg. aluminum produced)					
	Calculated by Model				Experimental Correlations	
	Vaporization	Entrainment	HF	Total	Haupin	Henry
0.1	7.24	3.4	5.45	16.10	8.73	20.16
0.25	"	"	5.75	16.39	9.28	20.46
0.5	"	"	6.25	16.89	10.18	20.96
0.75	"	"	6.75	17.39	11.09	21.46
1.0	"	"	7.24	17.89	11.99	21.96
1.5	"	"	8.24	18.88	13.80	22.96
2.0	"	"	9.24	19.88	15.61	23.96

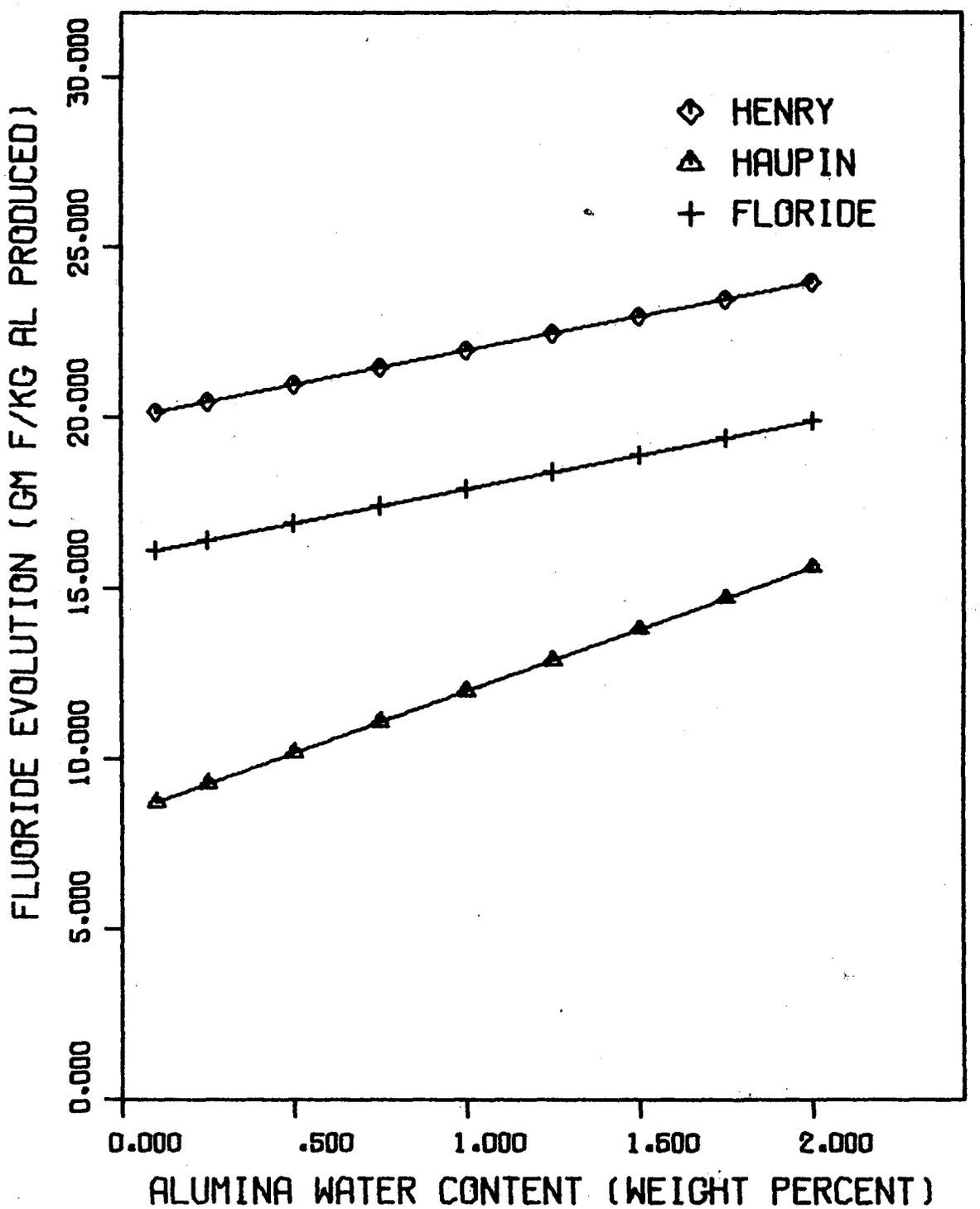

Figure 12

Fluoride Evolution as a Function of Alumina Water Content Using Assumption that 5 Percent of Alumina Moisture Reacts. Refer to Table 18 for Other Assumptions Used.

TABLE 19

Calculated Water Content of Alumina Containing 2% Moisture (by weight) after Heating 1 hour.[25]

Temp. K	Water Content, Wt.%
298	2.0
473	1.2
573	0.9
673	0.8
773	0.6
873	0.3
973	0.05

These data and the experiments of Henry would seem to indicate that the temperature required to achieve 0.1% water as suggested by Grjotheim would be at least 150 K higher than that normally present on the crust, about equal to the temperature Henry used to calcine ore for his experiment. Therefore it is reasonable to expect that the alumina would have a higher water content when it enters the cell. Since, as pointed out by Henry, reaction of 0.2 to 0.5% water to produce HF would result in a value for this fume that would greatly exceed measured values, this gives additional support to the hypothesis that some kinetics is involved.

In summary, the use of the optional treatment of alumina moisture assuming that 5% of the moisture reacts appears to be the more justifiable, both from the results of the model as well as consideration of the expected water content of alumina under normal cell conditions, than the standard model assumption.

Items for Future Work

Vaporization

It is apparent that due to the disagreement between the two sets of vapor pressure data used in this model, further work is needed to identify an optimum correlation for vapor pressure of the bath as a function of temperature and composition.

During the course of this investigation, other sets of vapor pressure data were investigated. The data of Rolin and Houriez,[20] Mesrobian, Rolin, and Pham,[21] and Gerlach, Hennig, and Mucke[22] appear to agree fairly well with Kuxmann and Tillessen's data, but do not cover the composition range of Vajna and Bacchiega's data, especially the effect of calcium fluoride additions. These encompass the readily available measurements that have been made within the last fifteen years.

In summary, if consistent data that both correlated well with other measurements and included the effects of varying alumina and calcium fluoride content were available, this would allow more accurate and comprehensive modelling of fluoride evolution due to vaporization of bath.

Entrainment

It is evident that the assumption made in the Procedure of a constant value for entrainment is at best an approximation, although the error involved may not be great if entrainment accounts for only 6 percent of fluoride evolution as indicated by Haupin's data. On the other hand a theoretical treatment of entrainment, taking into account

varying bubble and drop size, turbulence in the bath, cell crust openings, air velocity, etc. would be nearly impossible without making gross simplifications. Probably the best way to model this aspect of fluoride evolution is empirically by making extensive measurements of entrained fume as a function of bath temperature, cryolite ratio, and bath composition. One way to make these measurements might be to measure calcium content in the fume. Since the principal calcium containing species in the cell are essentially nonvolatile, calcium present in the fume can be assumed to be due to entrainment, and therefore the entrained fluoride would be proportional to the measured calcium content.

HF Evolution

Atmospheric Humidity Mechanism

The results of using this mechanism in the fluoride model would seem to indicate that although water in the potroom atmosphere does react to form HF, the reaction does not go to completion due to kinetic considerations. This possibility seems likely because there seem to be kinetic considerations involved in the reactions of the other two sources of water (anode hydrogen and alumina moisture), and it is possible that some of the same reaction mechanisms for water and fluorides forming HF are operative. For further work in this area, a study of the kinetics of the water-fluoride species reactions and of the transport mechanisms involved in introducing water from the atmosphere into the cell would allow a model of HF evolution due to hydrolysis of atmospheric moisture to be constructed that would correlate better with experimental findings.

With regard to experimental measurements, the experimental correlation of Haupin used for comparison is only a linear regression of data which shows a fair amount of scatter as mentioned in the introduction. Henry's data on the effect of humidity[14] also shows a great deal of scatter and little correlation possible, although in this case the range of humidities investigated was not great. Also, these measurements were made by analysis of scrubber brine from a continuous fume collection system rather than by directly sampling unburned fumes from the crust. Therefore secondary reactions had an opportunity to occur which would increase the amount of HF available through hydrolysis of aluminum fluoride, chiolite, and $NaAlF_4$ in the particulate fume.

Therefore, further measurements of HF content of unburned cell fumes as a function of humidity would be helpful in verifying the results of any further modelling of this mechanism.

Anode Hydrogen Mechanism

As previously discussed, there is definite indication that reaction kinetics need to be included in the model to obtain an optimum correlation with experimental results. The option used in the model assumed a constant factor of 0.4, that being the best available assumption with the limited data available. However, the assumption of a constant value here is most likely an oversimplification since elementary reaction kinetics suggests that the rate of HF formation will be a function of the rate constants for the reactions (and at least 2 reactions are probably involved here) which are, in turn,

usually exponential functions of temperature, and the concentrations of the reactant and product species. However, further refinement of this portion of the model to include reaction kinetics would be difficult to verify with the experimental data correlations used here.

There are two approaches that could be used to quantify the kinetics. One would be a theoretical approach involving experimental determinations of reaction rates and an analysis of the reaction steps involved. The other, and probably the most practical, would be to make extensive experimental measurements of HF evolution as a function of anode hydrogen content, perhaps using experimental cells for better control of cell parameters. The data could then be empirically fitted to a polynomial curve that would then be substituted into the model for the existing expression for HF evolution due to anode hydrogen.

Alumina Moisture Mechanism

The model results and comparison with the experimental correlations appear to justify the hypothesis that only about 5 percent of the moisture in the alumina after drying on top of the crust reacts to form HF. Henry's data indicate that this factor is relatively constant for varying alumina water contents. However, as noted in the discussion of the kinetic factor for anode hydrogen, this factor is also unlikely to be constant. Unfortunately, the data from Henry's measurements have too much scatter and too few points to allow a statistically valid correlation to be generated. Therefore the recommendations discussed for the anode hydrogen mechanism would also apply here--either an investigation of the kinetics or further empirical measurements. One point to be considered with respect to the kinetics

is that the final reactions with water to produce HF may be the same for all 3 mechanisms. Therefore a model for the kinetics of this phase of the mechanism may be applicable to all three. However, further investigation would be necessary to determine if this is the case.

Conclusions

1. The optimum correlation between the predictions of the fluoride model and the linear regression equations of experimental data on fluoride evolution occurred using the following model options:
   a) Bath vapor pressure data of Kuxmann and Tillessen when temperature and cryolite ratio were varied.
   b) Assumption of a kinetic factor for the anode hydrogen mechanism of HF generation.
   c) Assumption that alumina moisture reacts to the extent of about 5% of its concentration when on the crust.
2. No conclusion could be drawn as to whether the use of the entrainment value calculated from Haupin's or Less and Waddington's measurements produced the better results.
3. Use of the mechanism for HF generation from potroom atmospheric humidity gave results that indicated this mechanism was significant, but that the reaction did not go to equilibrium, and therefore a simple thermodynamic model of the mechanism is insufficient.
4. A correlation between predicted fluoride evolution and alumina and calcium fluoride content was possible by using the vapor pressure data of Vajna and Bacchiega. However, using this option, the model did not correlate well with experimental curves when alumina content, temperature, and cryolite ratio were varied.

5. Items for future work that would lead to improvements in the model include:

   a) An improved correlation between bath vapor pressure and composition.

   b) A measurement of entrained fume as a function of cell temperature and composition.

   c) An investigation of the kinetics of HF producing cell reactions or measurements of HF evolution as a function of atmospheric humidity, anode hydrogen, and alumina moisture content.

References

1. T. G. Pearson: The Chemical Background of the Aluminum Industry, p. 56. Royal Institute of Chemistry, London, 1955.

2. K. Grjotheim, H. Kvande, K. Motzfeldt, and B. J. Welch: "The Formation and Composition of the Fluoride Emissions from Aluminum Cells," Canadian Metallurgical Quarterly, 1972, Vol. 11, pp. 585-599.

3. S. S. Solntsev: "A Method of Determining Fluorine Balance in Aluminum Electrolysis," The Soviet Journal of Non-Ferrous Metals, 1967, Vol. 8, No. 2, pp. 74-76.

4. E. H. Howard: "Some Physical and Chemical Properties of a New Sodium Aluminum Fluoride," Journal of the American Chemical Society, 1954, Vol. 76, pp. 2041-2.

5. L. N. Sidorov, E. V. Erokhin, P. A. Akishin, and E. N. Kolosov: "Mass Spektrometricheskoe Issledovanie Sostava I Davleniya Para Sistemy NaF-AlF_3," Doklady Akademia Nauk, SSSR, 1967, Vol. 173, pp. 370-373.

6. E. W. Dewing: "The Chemistry of the Alumina Reduction Cell," Canadian Metallurgical Quarterly, 1974, Vol. 13, pp. 607-618.

7. L. N. Less and J. Waddington: "The Characterisation of Aluminum Reduction Cell Fume," Light Metals 1971, T. G. Edgeworth, ed., pp. 499-508, T.M.S.-A.I.M.E., New York, 1971.

8. W. E. Haupin: Unpublished Communication, Alcoa Laboratories, Alcoa Center, PA, 1976.

9. J. Miller: "Environmental Conditions Inside and Outside a Modern Aluminium Smelter at A/S Ardal og Sunndal Verk, Norway," Engineering Aspects of Pollution Control in the Metals Industries, pp. 165-172, The Metals Society, London, 1974.

10. G. Andes, F. Bjorke, and P. Farrier: "Hooding Efficiencies of Prebake Aluminum Cells--Bluff Smelter, New Zealand," Light Metals 1976, Vol. 2, pp. 467-499, T.M.S.-A.I.M.E., New York, 1976.

11. W. E. Haupin and W. C. McGrew: "See-Through Hall Heroult Cell," Aluminium Duesseldorf, 1975, Vol. 51, pp. 273-275.

12. R. H. Perry and C. H. Chilton: Chemical Engineers' Handbook 5th Ed., p. 18-65, McGraw-Hill, New York, 1970.

13. A. Vajna: "Tensioni Superficiali dei Bagni Criolitici allo Stato Fuso," Alluminio, 1951, Vol. 20, pp. 29-38.

14. J. L. Henry: "A Study of Factors Affecting Fluoride Emissions from 10,000 Ampere Experimental Aluminum Reduction Cells," Extractive Metallurgy of Aluminum, Vol. 2, G. Gerard ed., pp. 67-81, Interscience, New York, 1963.

15. A. A. Kostyukov: Tsvetnye Metally, 1963, Vol. 36, p. 38.

16. M. C. Richard: "Use of a Mathematical Cell Model to Determine Cell Parameter Design Changes for Production Maximization," Light Metals 1975, Vol. 1, pp. 95-109, T.M.S.-A.I.M.E., New York, 1975.

17. D. R. Morris, "A Mathematical Model of the Aluminum Reduction Cell," Canadian Metallurgical Quarterly, Vol. 14, p. 169, 1975.

18. B. Berge, K. Grjotheim, C. Krohn, R. Neumann, and K. Tørklep: "Operational Characteristics and Current Efficiency of Aluminum Reduction Cells," Light Metals 1975, Vol. 1, pp. 37-43, T.M.S.-A.I.M.E., New York, 1975.

19. U. Kuxmann and U. Tillessen: "Damfdruckmessungen in den Systemen NaF-$A\ell F_3$ und LiF-NaF-$A\ell F_3$," Erzmetall, 1967, Vol. 20, pp. 147-155.

20. M. Rolin and J. Houriez: Bulletin du Societe Chimique de France, 1964, p. 891.

21. G. Mesrobian, M. Rolin, and H. Pham: "Etude Sous Pression des Melanges Fluorure de Sodium Fluorure D'Aluminium Riches en Fluorure D'Aluminium," Revue Internationale des Hautes Temperatures Refractes, 1972, Vol. 9, pp. 139-146.

22. G. Gerlach, V. Hennig, and M. Mucke: "Dampfdruckmessungen an NaF-$A\ell F_3$-$A\ell_2O_3$-$A\ell$ Schmelzen," Erzmetall, 1973, Vol. 26, pp. 496-501.

23. A. D. Romig, Jr.: The Fundamentals of Engineering Statistics, 2nd Ed., p. 16, Lehigh University, Bethlehem, Pa. 1976.

24. A. Vajna and R. Bacchiega: "Tensione di Vapore dei Bagni Criolitici Struttura dei Bagni Criolitici allo Stato Solido, Liquido, di Vapore," Metallurgia Italiana, 1960, Vol. 52, pp. 481-494.

25. C. Cochran, W. Sleppy, and W. Frank: "Fumes in Aluminum Smelting: Chemistry of Evolution and Recovery," Journal of Metals, 1970, Vol. 22, pp. 54-57.

26. O. Kubaschewski, E. Evans, and C. Alcock: Metallurgical Thermochemistry, 4th Ed., Pergamon Press, Oxford, 1967.

27. M. Vetyukov and N. Van Ban: "Alumina Activity in Ternary System Na_3AlF_6-AlF_3-Al_2O_3," The Soviet Journal of Nonferrous Metals, 1971, Vol. 12, pp. 35-36.

28. A. Sterten and K. Hamberg: "The NaF-Al_2O_3-Na_2O System--Activities of Aluminium Fluoride and Sodium Fluoride in Melts Saturated with Alumina," Light Metals 1976, Vol. 1, pp. 203-221, T.M.S.-A.I.M.E. New York, 1976.

29. Dow Chemical Company Thermal Research Laboratory: JANAF Thermochemical Tables, 2nd Ed. US National Bureau of Standards, Washington, 1971.

APPENDIX 1 - List of Symbols

Symbol	Definition	Units
A	Kuxmann and Tillessen vapor pressure coefficients	none
AALF3	Raoultian activity of AlF_3	none
AAL2O3	Raoultian activity of Al_2O_3	none
ACONS	Anode consumption	kg anode/kg Al
AE	Anode effect flag (1=Anode Effect)	none
B	Kuxmann and Tillessen vapor pressure coefficients	none
CE	Current efficiency	amperes/ampere
CRATIO	Cryolite ratio	moles NaF/moles AlF_3
DGHYD	Standard Gibbs Free Energy of hydrolysis reaction	joules
FDIMER	Fraction of dimer in vapor	none
FK	Kinetic factor for anode hydrogen	none
FVP	Vapor pressure factor	none
HCONTNT	Anode hydrogen content	g. hydrogen/g. carbon
II	Input device logical unit number	none
IO	Output device logical unit number	none
IRUN	Flag to set switches on first run	none
KHYD	Equilibrium constant for hydrolysis	none
KVAPR	Equilibrium constant for vaporization of electrolyte	none
MSW	Option switch matrix	none
NAL2O3	Al_2O_3 concentration in bath	weight percent
NANGAS	Moles anode gas	moles gas/kg. Al

NCAF2	CaF_2 concentration in bath	weight percent
NH2OH	Moisture due to anode hydrogen	moles H_2O/kg. Al
NH2OW	Moisture due to alumina feed	moles H_2O/kg. Al
NLIF	LiF concentration in bath	weight percent
NMGF2	MgF_2 concentration in bath	weight percent
PAH	Atmospheric humidity	pascals
PHF	Partial pressure of HF	none
PH2O	Partial pressure of water vapor	none
PTOTAL	Atmospheric pressure	pascals
PVAPR	Vapor pressure above cryolite bath	atmospheres
R	Gas constant	joule/mole-^oK
T	Bath temperature	kelvin
TR	Ore feeding flag (1=feeding)	none
VB	Intermediate calculation	-
WCA	Water content of alumina	weight percent
WCAD	Water content of alumina after drying	weight percent
WF	Total fluoride evolution predicted by model	g. F/kg. Al
WFALC	Fluoride evolution predicted by Haupin's equation	"
WFENTR	Fluoride evolution in model due to entrainment	"
WFHEN	Fluoride evolution predicted by Haupin's regression of Henry's data	"
WFHF	Fluoride evolution in model due to HF generation	"
WFSOL	Fluoride evolution predicted by Solntsev's equation	"

WFVAPR	Fluoride evolution in model due to bath vaporization	g.F./kg. Al

APPENDIX 2 - Source Listing of

Fluoride Evolution Model 'FLORIDE'

```
      SUBROUTINE FLORIDE (CRATIO,NANGAS,ACONS,NAL2O3,
     1  NCAF2,NMGF2,NLIF,T,PAH,HCONTNT,CE,WCA)
C...
C...     SUBROUTINE ≠FLORIDE≠ CALCULATES THE FLUORIDE
C...     EVOLUTION FROM THE CELL.
C...
C...
C...     DECLARATIONS
      REAL NANGAS,NAL2O3,KHYD,KVAPR
      REAL NCAF2,NMGF2,NLIF,NH2O,NH2OH,NH2OW,NHF
      DIMENSION MSW(5)
C...
C...     INITIALIZE VARIABLES
      DATA II,IO,IP / 5,6,7 /
      DATA R,PTOTAL / 8.3144, 101325.0 /
      DATA IRUN / 0 /
      WRITE (IO,100)
  100 FORMAT (3/,2X,10(1H.),18HFLUORIDE EVOLUTION,
     1   20H (GM/KG AL PRODUCED) ,70(1H.),2/)
      WRITE (IO,104) T,PAH,HCONTNT,WCA
  104 FORMAT (5X,2HT=,F6.0,2X,14HHUMIDITY (PA)= ,F8.1,
     1   2X,10HH CONTENT= ,F8.4,2X,14HWATER CONTENT= ,
     2   F6.2,1/)
      IF (IRUN.EQ.1) GO TO 5
      READ (II,200) (MSW(I),I=1,5)
  200 FORMAT (5(I1,1X))
      WRITE (IO,105) (MSW(I),I=1,5)
  105 FORMAT (5X,11HSWITCHES -  ,5(I1,1X))
    5 CONTINUE
      IRUN=1
C...
C...     BEGIN CALCULATIONS
C...
C...     CALCULATE FLUORIDE DUE TO HF GENERATION
C...
C...          CALCULATE WATER FROM ALUMINA FEED
      NH2OW=0.
      IF (MSW(1).EQ.1) GO TO 11
      IF (MSW(1).EQ.2) GO TO 12
      GO TO 14
   11 WCAD=0.05*WCA
      GO TO 13
   12 WCAD=WCA
      IF (WCA.GT.0.1) WCAD=0.1
   13 NH2OW=18.8889*WCAD/18.015
C...
C...          CALCULATE WATER FROM ANODE HYDROGEN
   14 FK=0.
      IF (MSW(2).EQ.1) FK=1.0
      IF (MSW(2).EQ.2) FK=0.4
      NH2OH=ACONS*HCONTNT*FK*1000./2.016
C...
C...          CALCULATE HF PARTIAL PRESSURE
C...          DUE TO HUMIDITY
      PHF=0.
      IF (MSW(3).EQ.0) GO TO 19
      PH2O=PAH/PTOTAL
      AAL2O3=(-3.4218E-4*NAL2O3**3+0.013506*NAL2O3**2
     1   -0.031509*NAL2O3+6.1619E-3)*(-2.0*CRATIO+7.)
      AALF3=10.**(0.2551*(CRATIO**2)-2.105*CRATIO
```

```
     1    +0.6625)
      DGHYD=130130.-14.38*T*ALOG10(T)-87.89*T+3.27E-3
     1    *T*T+1.7E5/T
      KHYD=EXP(-DGHYD/(R*T))
      PHF=SQRT(AALF3**(2./3.)* PH2O*KHYD/AAL2O3
     1    **(1./3.))
C...
C...            CALCULATE TOTAL HF EVOLUTION
   19 WFHF=18.998*(PHF*NANGAS+2.*(NH2OW+NH2OH))
C...
C...     CALCULATE FLUORIDE DUE TO VAPORIZATION
      WFVAPR=0.
      IF (MSW(4).EQ.1) GO TO 21
      IF (MSW(4).EQ.2) GO TO 22
      GO TO 29
   21 FVP=0.6
      A=950.86*CRATIO+7537.4
      B=0.21974*CRATIO+8.0099
      PVAPR=(10.**(-A/T+B))/760.
      GO TO 28
   22 FVP=1.0
      VB=10.168-11105.8*(1./(T))-0.03438*NAL2O3-0.03302
     1    *NCAF2-0.37494*CRATIO
      PVAPR=(10.**VB)/760.
   28 KVAPR=10.**(9300./T-5.9)
      FDIMER=(2.*KVAPR*PVAPR+1.-SQRT(4.*KVAPR*PVAPR
     1    +1.0))/(2.0*KVAPR*PVAPR)
      WFVAPR=FVP*PVAPR*NANGAS*(1.+FDIMER)*75.99
C...
C...     CALCULATE FLUORIDE DUE TO ENTRAINMENT
   29 CONTINUE
      WFENTR=0.
      IF (MSW(5).EQ.1) WFENTR=3.4
      IF (MSW(5).EQ.2) WFENTR=1.5
C...
C...     CALCULATE TOTAL FLUORIDE EVOLUION
      WF=WFVAPR+WFENTR+WFHF
C...
C...     CALCULATE VALUE PREDICTED FROM SOLNTSEV
      WFSOL=279./(CRATIO**2)+0.047*(T-273.)-61.
C...
C...     CALCULATE PREDICTED VALUE FROM ALCOA FORMULA
      AE=0.0
      TR=0.0
      WFALC=-156.5-27.0*CRATIO+0.244*(T-273.)+0.00377
     1    *PAH+3.62*WCA-1.29*NAL2O3+13.5*AE+2.6*TR+960.0
     2    *HCONTNT
C...
C...     CALCULATE VALUE PREDICTED FROM HENRY
      WFHEN=(-42518.+929.*CRATIO-254.5*CRATIO**2-41.03
     1    *NAL2O3+0.914*NAL2O3**2+25.18*(T-273.16)+
     2    1.744E7/(T-273.16))*(4.71/(CE*100.))+2.*WCA
C...
      WRITE (IO,102)
  102 FORMAT (7X,5HVAPOR,7X,7HENTRAIN,7X,6HHF GEN,7X,
     1    5HTOTAL,7X,7HSOL EQN,6X,5HALCOA,8X,5HHENRY,1/)
      WRITE (IO,103) WFVAPR,WFENTR,WFHF,WF,WFSOL,WFALC
     1    ,WFHEN
  103 FORMAT (7(5X,F7.3,1X))
      RETURN
      END
```

Vita

Jonathan Patrick Dandridge was born on October 6, 1949 in Rochford, Essex, England to Peter F. and Peggy K. Dandridge. Mr. Dandridge moved with his family to Boston, Massachusetts in December 1961. In June 1967, he graduated from Roxbury Latin School in West Roxbury, Massachusetts and in September of 1967 he entered Lehigh University. He graduated from Lehigh in June 1971 with the degree of Bachelor of Science in Metallurgy and Materials Science. In October 1971, Mr. Dandridge entered the United States Air Force serving as a Second Lieutenant with the Air Force Communications Service. During this time he studied for and obtained the degree of Master of Business Administration from Eastern New Mexico University, Portales, New Mexico, in August 1975. In October of 1975, he separated from the Air Force with the rank of Captain.

From January 1976 to the present Mr. Dandridge has been enrolled in the Department of Metallurgy and Materials Science at Lehigh University.